Journal for ImmunoTherapy of Cancer

Novel oncolytic adenovirus expressing enhanced cross-hybrid IgGA Fc PD-L1 inhibitor activates multiple immune effector populations leading to enhanced tumor killing in vitro, in vivo and with patient-derived tumor organoids

Firas Hamdan ,[1,2,3] Erkko Ylösmäki ,[1,2,3] Jacopo Chiaro,[1,2,3] Yvonne Giannoula,[1] Maeve Long,[4] Manlio Fusciello ,[1,2,3] Sara Feola ,[1,2,3] Beatriz Martins,[1,2,3] Michaela Feodoroff,[1,2,3] Gabriella Antignani,[1,2,3] Salvatore Russo,[1,2,3] Otto Kari,[3] Moon Hee Lee,[2,5] Petrus Järvinen,[6] Harry Nisen,[6] Anna Kreutzman,[1,2,3] Jeanette Leusen ,[7] Satu Mustjoki ,[2,5,8,9] Thomas G McWilliams,[4,10] Mikaela Grönholm,[1,2,3,8] Vincenzo Cerullo [1,2,3,8,11]

To cite: Hamdan F, Ylösmäki E, Chiaro J, *et al*. Novel oncolytic adenovirus expressing enhanced cross-hybrid IgGA Fc PD-L1 inhibitor activates multiple immune effector populations leading to enhanced tumor killing in vitro, in vivo and with patient-derived tumor organoids. *Journal for ImmunoTherapy of Cancer* 2021;**9**:e003000. doi:10.1136/jitc-2021-003000

► Additional supplemental material is published online only. To view, please visit the journal online (http://dx.doi.org/10.1136/jitc-2021-003000).

EY and JC contributed equally.

Accepted 21 July 2021

For numbered affiliations see end of article.

Correspondence to
Professor Vincenzo Cerullo; vincenzo.cerullo@helsinki.fi

ABSTRACT

Background Despite the success of immune checkpoint inhibitors against PD-L1 in the clinic, only a fraction of patients benefit from such therapy. A theoretical strategy to increase efficacy would be to arm such antibodies with Fc-mediated effector mechanisms. However, these effector mechanisms are inhibited or reduced due to toxicity issues since PD-L1 is not confined to the tumor and also expressed on healthy cells. To increase efficacy while minimizing toxicity, we designed an oncolytic adenovirus that secretes a cross-hybrid Fc-fusion peptide against PD-L1 able to elicit effector mechanisms of an IgG1 and also IgA1 consequently activating neutrophils, a population neglected by IgG1, in order to combine multiple effector mechanisms.

Methods The cross-hybrid Fc-fusion peptide comprises of an Fc with the constant domains of an IgA1 and IgG1 which is connected to a PD-1 ectodomain via a GGGS linker and was cloned into an oncolytic adenovirus. We demonstrated that the oncolytic adenovirus was able to secrete the cross-hybrid Fc-fusion peptide able to bind to PD-L1 and activate multiple immune components enhancing tumor cytotoxicity in various cancer cell lines, in vivo and ex vivo renal-cell carcinoma patient-derived organoids.

Results Using various techniques to measure cytotoxicity, the cross-hybrid Fc-fusion peptide expressed by the oncolytic adenovirus was shown to activate Fc-effector mechanisms of an IgA1 (neutrophil activation) as well as of an IgG1 (natural killer and complement activation). The activation of multiple effector mechanism simultaneously led to significantly increased tumor killing compared with FDA-approved PD-L1 checkpoint inhibitor (Atezolizumab), IgG1-PDL1 and IgA-PDL1 in various in vitro cell lines, in vivo models and ex vivo renal cell carcinoma organoids. Moreover, in vivo data demonstrated that Ad-Cab did not require CD8 + T cells, unlike conventional checkpoint inhibitors, since it was able to activate other effector populations.

Conclusion Arming PD-L1 checkpoint inhibitors with Fc-effector mechanisms of both an IgA1 and an IgG1 can increase efficacy while maintaining safety by limiting expression to the tumor using oncolytic adenovirus. The increase in tumor killing is mostly attributed to the activation of multiple effector populations rather than activating a single effector population leading to significantly higher tumor killing.

INTRODUCTION

Immune checkpoint inhibitor (ICI) therapies have been established as a potent treatment option for a plethora of tumor types and have significantly expanded the therapeutic armamentarium in oncology. Such agents target immune inhibitory receptors and interrupt coinhibitory signaling pathways, abrogating their immunosuppressive function and consequently revitalizing antitumor immune response. The consequent restoration of immune-mediated elimination of tumor cells leads to long-term, sustained tumor responses,[1 2] resulting in their approval as first-line treatments for a growing list of malignancies.[3] Nevertheless, accumulating evidence indicate that checkpoint inhibitors can only benefit a fraction of patients.[4]

In spite of such limitations, there has been a shift of focus in improving ICIs therapeutic efficacy. All clinically approved ICIs are antibodies that primarily act as antagonizing agents with their main mechanism of action being the reconstitution of a T-cell response by disrupting an immunosuppressive axis.[5] Nevertheless, ICIs are either limited or entirely not able to elicit crucial antibody-dependent effector mechanisms[6] such as complement-dependent cytotoxicity (CDC) or antibody-dependent cell cytotoxicity/phagocytosis (ADCC/ADCP) which are pertinent to an antibody. Based on clinical data, activation of effector mechanisms are a necessity for therapeutic antibodies to achieve tumor clearance.[7] Moreover, effector mechanisms such as ADCC and CDC have been noticed to be an essential requirement for enhanced antitumor responses for some modified ICIs against CTLA-4[8] or PD-L1.[9 10] Thus, equipping or enhancing ICIs with such effector mechanism via the Fc-fragment may lead to improved efficacy, resulting in higher response rates in the clinic.

In the clinic, all therapeutic antibodies against cancer are of the IgG isotype and predominantly of the IgG1 subtype. This is primarily due to the ability of an IgG to activate the complement system and natural killer cells (NK), leading to tumor killing. Yet, IgG fails to efficiently activate the most abundant leukocyte population able to infiltrate solid tumors, neutrophils. This is mostly due to the relatively high expression of inhibitory Fc-γIIB (CD32B)[11] and Fc-γIIIB (CD16B),[12] which do not contain any signaling motif yet has been seen to block the activation of ADCC.[13] In order to capitalize on such a promising population, IgA antibodies have been used since they bind to the Fc-α receptor, CD89, which is highly expressed on neutrophils, monocytes and macrophages consequently eliciting ADCC or ADCP.[14 15] In addition, the Fc-α-mediated activation of neutrophils by IgA antibodies has been shown to be more effective in tumor killing than the Fc-γ-mediated effector mechanisms by IgG antibodies in multiple types of cancers.[16] However, it has been shown that the addition of both IgG and IgA antibodies further enhances tumor cytotoxicity.[17]

Here, we have developed a Fc-fusion peptide against PD-L1 consisting of a cross-hybrid Fc region containing constant regions of an IgG1 and an IgA1, termed IgGA,[18] connected to a PD-1 ectodomain, carrying mutations that increase its affinity towards PD-L1 via a glycine linker. However, carrying a competent/functional Fc region can be a double-edged sword since immune checkpoints are expressed ubiquitously and such antibodies are systemically administered, frequently causing irAEs.[19] To circumvent this obstacle, we limited the expression of the Fc-fusion peptide directly into the tumor microenvironment by cloning it into an oncolytic adenovirus. Oncolytic viruses have become ideal gene therapy vehicles because they are able to selectively infect and kill tumor cells while leaving healthy tissues intact, as shown in preclinical trials and patients.[20] Moreover, preclinical and clinical research has demonstrated that these agents specifically express their transgenes to the tumor microenvironment with limited leakage.[21 22]

We demonstrated that the cross-isotype Fc region gives the ICI the ability to elicit effector mechanisms of both an IgA and an IgG isotype in various tumor cell lines. The subsequent activation of multiple effector mechanisms further enhanced tumor killing and was shown to be superior than a PD-L1 IgG1 antibody or Atezolizumab, a currently approved FDA ICI. To further evaluate the efficacy of the Fc fusion peptide, we tested our engineered adenovirus (named Ad-Cab) in multiple in vivo tumor models and showed significantly enhanced tumor growth control as compared with unarmed adenovirus or ICI against murine PD-L1. Finally, to examine the oncolytic efficacy of the Ad-Cab in a testing platform with high clinical response predictability, we used renal cell carcinoma patient-derived organoids (RCC PDO). In this model, we showed significantly enhanced tumor cell lysis as compared with Atezolizumab or an anti-PD-L1 IgG antibody with functional Fc region.

Cell lines and antibodies

Human lung cancer cell line A549 ((ATCC Cat# CRM-CCL-185, RRID:CVCL_0023), human breast cancer cell line MDA-MB-436 ((ATCC Cat# HTB-130, RRID:CVCL_0623), murine colon adenocarcinoma CT26 (ATCC Cat# CRL-2638, RRID:CVCL_7256), murine breast cancer cell line 4T1 (ATCC Cat# CRL-2539, RRID:CVCL_0125) and murine skin cancer cell lines B16F1 (ATCC Cat# CRL-6323, RRID:CVCL_0158) and B1610 (ATCC Cat# CRL-6475, RRID:CVCL_0159) were purchased from the American Type Culture Collection (ATCC) after 2013. Cell lines were thawed at passage 5 and kept in culture until reaching passage 15. All cell lines were authenticated by the ATCC, cultured under appropriate conditions and regularly checked for mycoplasma contaminations. Atezolizumab and IgG1-PD-L1 were purchased from Invivogen. IgA-PD-L1 was kindly provided by Dr Jeanette Leusen of Utrecht University Medical University.

Preparation of conditionally replicating adenovirus and transgene modifications

All adenoviruses were generated as conditionally replicating adenoviruses using standard protocols previously described.[23] Ad-Cab and unarmed viruses are of the chimeric 5/3 serotype with a 21-nucleotide deletion in the E1A region resulting in selective replication in Rb-deficient pathway cells. Ad-RFP has the same genetic modification in E1A but originates from the serotype 5. All transgenes were cloned by replacing the gp19K+7.1K region in the E3 gene using Gibson-Assembly previously described.[24]

Generation of Fc-fusion peptide

The Fc-Fusion peptide consists of a chimeric Fc containing constant domains of an IgG1 and IgA connected to an enhanced PD-1 ectodomain via five GGGS linkers. The

cross-hybrid Fc has been described[18] as well as the PD-1 ectodomain.[25]

Cell viability assays

A total of 10,000 cells were plated in a 96-well plate overnight and subsequently infected at different MOIs. Three-day postinfections cell viability was determined by MTS according to the manufacturer's protocol (Cell Titer 96 AQueous One Solution Cell Proliferation Assay; Promega, Nacka, Sweden). Spectrophotometric data were acquired with Varioskan LUXMultimode Reader (Thermo Scientific, Carlsbad, C, USA) operated by SkanItsoftware.

Competition assay

A total of 100,000 A549 cells were plated in a 96-well, washed with PBS and incubated with various concentrations of purified Fc-fusion peptide for 45 min on ice. Next, 10 ug/mL of Atezolizumab (Invivogen, Cat# hpdl1-mab12) was added and incubated for 30 min on ice. Atezolizumab was then detected by staining with a PE labeled antihuman IgG (BioLegend Cat# 409303, RRID:AB_10900424). Cells where then washed and resuspended in PBS. Competition was then quantified by flow cytometry using the BD Accuri 6 plus (BD Biosciences) and analyzed using the FlowJo software (FlowJo, V.10.7.1, RRID:SCR_008520).

PBMCs, PMN and serum collection

A total of 40 mL of blood was collected from healthy volunteers in BD Vacutainer collection tubes (BD Bioscience) and allowed to clot for 30 min at room temperature. After clotting, clots were removed, and samples centrifuged for 5 min at 2500 rpm. Separated serum was collected and samples from 15 volunteers were pooled together. Polymorphonuclear cells (PMNs) and peripheral blood mononuclear cells (PBMCs) were isolated from buffy coats as previously described.[18] The PBMC and PMN layers were subsequently removed between serum and Ficoll or in the Histopaque layer, respectively, and cultured in 1xRPMI (Roswell Park Memorial Institute, Gibco, Cat# 21875034)-

Mixed leukocyte reaction

Monocytes were first isolated from PBMCs as previously described. Following isolation, monocytes were differentiated using DMEM low glucose supplemented with 10% FBS, 500 U/mL of IL-4 (PeproTech, #200–04) and 250 U/mL of GM-CSF (Adcam, ab88382) for 7 days. PBMCs from a different donor were freshly isolated, labeled with CFSE and incubated with monocyte-derived dendritic cells for 5 days at a ratio of 1:10 in the presence of 1 µg/mL of Atezolizumab or isolated IgGA Fc-fusion peptide. Cells from the supernatant were then collected and using flow-cytometry CFSE was measured in CD3 + CD8+ T cells.

Complement-dependent cytotoxicity assay

A total of 100,000 cancer cells were plated per well to a 96-well plate and infected with 10 or 100 MOI of virus for 48 hours at 37°C. Then, complement active pooled human serum or heat inactivated serum (by incubating serum at 56°C for 30 min) was added to a final concentration of 15.5% and incubated for 4 hours. Subsequently, lysis was quantified by washing cells and stained with 7-amino-actinomycin D (7-AAD) (eBioscience, Cat# 00-6993-50) and measured by flow cytometry.

Antibody-dependent cell cytotoxicity assays

ADCC assays were performed through measuring cell killing by determining the amount of LDH released using a colometric assay (CyQUANT LDH Cytotoxicity Assay, Cat# C20303). A total of 15,000 cells were then seeded and infected with 10 or 100 MOI of virus for 48 hours at 37°C. Afterwards, PBMCs or PMNs were added in a 100:1 or 40:1 ratio (E: T), respectively, and incubated for 4 hours at 37°C. LDH was measured using the mentioned kit and percent cytotoxicity was calculated as follows: Percent cytotoxicity = ("experimental" – "effector plus target spontaneous")/("target maximum" – "target spontaneous") × 100%, where "experimental" corresponds to the signal measured in a treated sample, "effector plus target spontaneous" corresponds to the signal measured in the presence of PMN or PBMC and tumor cells alone and "target maximum" corresponds to the signal measured in the presence of detergent lysed tumor cells

Antibody-dependent cell phagocytosis

Around 2,000,000 freshly isolated PBMCs were cultured in a T25 culture flask for 2 hours at 37°C. Floating cells were removed, and adherent monocytes were differentiated into macrophages by culturing in RPMI supplemented with 50 µg/mL of M-CSF (Sigma Aldrich, Cat# M6518) for 7 days at 37°C. 10,000 cells were incubated and infected with indicated viruses at 10 and 100 MOI for 48 hours. Cells were then labeled with CFSE (ThermoFisher), according to the manufactures instructions and monocyte-differentiated macrophages were added at a 5:1 effector:target ratio. After 4 hours, supernatant containing macrophages were removed and CFSE was measured using flow cytometry.

Trogocytosis

Trogocytosis was performed as previously described.[26] In brief, 5000 cells were infected with 100 MOI of virus and incubated for 48 hours at 37°C. Cell's lipid membrane were labeled with 5 um of DiO (ChemCruz, Cat# sc-214168), a lipophilic membrane dye, for 30 min at 37°C. Cells were washed and incubated with PMNs at a 40:1 (E:T) ratio. Samples were fixed using Paraformaldehyde (Sigma Aldrich) and measured using flow cytometry. Trogocytosis was measured by first gating on the neutrophil population and measuring the mean fluorescent intensity (MFI) of cells positive for DiO.

Real-rime quantitative analysis (xCELLigence assay)

The ability to induce ADCC was analyzed using the impedance-based real-time cytotoxicity assay with the xCELLigence system (ACEA Biosciences, San Diego,

California, USA). In each well, 25,000–100,000 cells were plated for 24 hours. Five µg/mL of designated antibody or purified Fc-fusion peptide was added along with PBMCs and PMNs at a 10:1 and 4:1 effector:target ratio. Cell index was measured every 5 min for a period of 6 hours. Killing rate was obtained by constructing a linear trendline and calculating the slope.

Live cell imaging

Imaging target to effector cell contacts, 15,000 A549 cells were plated per well of a 24 well plate (Corning) overnight. Cells were imaged for 30 min and subsequently treated with 10 µg/mL of indicated Fc-fusion peptides and PBMCs were added at 10:1 E:T ratio. The videos were acquired using an ANDOR Spinning Disc Microscope equipped with a Zyla camera (SR Apochromat ×100 objective, NA 1.49). Images were acquired every 5 min over the course of 2 hours 20 min.

Live-cell killing assay was performed by plating 100,000 A549 cells per well of a 24 well plate (Corning) overnight. Fifteen minutes prior to imaging, cells were incubated with 3 µM of Incucyte Caspace3/7 green apoptosis assay reagent (Sartorius, Cat# C10423). Cells were imaged using the IncuCyte S3 live cell analysis system equipped with a 10× air objective for a total of 24 hours. Images were acquired every 15 min and four fields of view were imaged per well. After 1 hour of imaging, cells were treated with indicated antibodies at 5 µg/mL and PMNs and PBMCs were added at 100:1 and 40:1 E:T ratios, respectively. Treated cells were returned to the IncuCyte S3 and imaged for the remainder 23 hours. Videos were processed with the IncuCyte analysis software (IncuCyte Chemotaxis Software, RRID:SCR_017316) and are displayed as four fields of view per second.

Whole blood assay

Blood was collected from three healthy volunteers in BD Vacutainer Heparin plasma tubes. A total of 200 µL of unprocessed blood was then incubated with 20 µg/mL of Traztuzumab or IgGA Fc-fusion peptide for 24 hours. After incubation, samples were treated with ACK lysing buffer (Gibco) to remove red blood cells. Cells were then stained with CD3, CD15, CD14, CD56 and CD11c to determine immune cell populations. Absolute numbers were calculated by using precision count beads (Biolegend, Cat# 424902) and following the manufacturers instructions.

Renal cell carcinoma patient-derived samples and ethical considerations

Renal cell carcinoma samples were obtained from four patients that underwent surgical removal of the tumors. Tumor samples were collected and delivered directly from the Peijas Hospital. The study was conducted in accordance with the declaration of Helsinki and patients gave their written consent.

Syngeneic animal experiments

All animal experiments were reviewed and approved by the Experimental Animal Committee of the University of Helsinki and the Provincial Government of Southern Finland (license number ESAVI/11895/2019). Around 4–6-week-old immunocompetent female BALB/c mice, purchased from Envigo (Venray, Netherlands), injected in the right flank with either 500,000 CT26 cells or 300,000 4T1 cells and were treated 7, 9, 11, 13, 19 and 21-days post-tumor implantation with 1×10^9 viral particles of virus intratumorally or 100 µg/mL of mPD-L1 (Bio X Cell Cat# BE0101, RRID:AB_10949073) intraperitoneally. Viral treatments were administered in 25 µL volume while antibodies were given in 100 µL. Tumor size was measured every second day and calculated using the following formula: (long side)×(short side)^2/2. Mice were sacrificed when any side of the tumor reached 16 mm.

As for in vivo CD8 depletion, mice were initially injected intraperitoneally with 500 µg of depleting CD8 antibody (Bio X Cell Cat# BE0061, RRID:AB_1125541) 1 day prior to treatment and then 100 µg every 2 days for the duration of the experiment.

At day 23 (CT26) and 15 (4T1) post-tumor implantation, two animals from each group were sacrificed and blood and tumors were collected. Blood was allowed to clot, then centrifuged at 500 g for 15 min and serum was subsequently collected. Tumors were crushed through a 0.22 µm cell strainer, centrifuged at 500 g for 10 min and supernatant collected. His-tagged proteins from serum and tumor supernatant was tested using a His-tag ELISA kit (Cell Biolabs, Cat#AKR-130).

Immune deficient NS (NOD/SCID) mice

Four–six-week-old Nod.CB17-Prkdc^{scid}/NCrCrl mice were purchased from Charles River and were injected with $5x10^6$ A549 cells in the right flank. Subsequently, 5×10^6 freshly isolated PBMCs were then injected intraperitoneally. After tumors were palpable, mice were treated two times (with a 3-day break in between) with 1×10^8 viral particles intratumorally.

Flow cytometry analysis

Flow cytometry analysis was done with either BD Accuri 6 plus (BD Bioscience) or Fortessa (BD Bioscience). Antibodies used include APC antimouse Ly6C (BioLegend Cat# 128015, RRID:AB_1732087), FITC antimouse NK1.1 (Thermo Fisher Scientific Cat# 11-5941-85, RRID:AB_465319), PE antimouse PD-1 (BioLegend Cat# 135206, RRID:AB_1877231), PE anti-Ly6G (BD Biosciences Cat# 551461, RRID:AB_394208), PerCP Cy5.5 antimouse CD11b (Thermo Fisher Scientific Cat# 45-0112-82, RRID:AB_953558), BV650 antimouse F4/80 (BD Biosciences Cat# 743282, RRID:AB_2741400), PeCy7 antimouse CD4 (Thermo Fisher Scientific Cat# 25-0041-82, RRID:AB_469576), PerCp/Cy5.5 antimouse CD107a (BioLegend Cat# 121626, RRID:AB_2572055), Pacific Blue antimouse CD3 (BioLegend Cat# 100214, RRID:AB_493645), PECy7 antimouse CD11c (Thermo

Fisher Scientific Cat# 25-0114-82, RRID:AB_469590), FITC antihuman CD56 (BioLegend Cat# 304604, RRID:AB_314446), PerCP antihuman CD8alpha (BioLegend Cat# 300922, RRID:AB_1575072), PE-Cy5 antihuman CD4 (Thermo Fisher Scientific Cat# 15-0049-42, RRID:AB_1582251), PE-Cy7 antihuman CD3 (BioLegend Cat# 300316, RRID:AB_314052), Pacific blue antihuman PD-1 (BioLegend Cat# 329915, RRID:AB_1877194), APC antihuman CD107a (BioLegend Cat# 328620, RRID:AB_1279055), APC antihuman CD11c (BioLegend Cat# 371505, RRID:AB_2616901), Pacific Blue antihuman CD15 (BioLegend Cat# 323021, RRID:AB_2105361) and PE antihuman CD14 (BioLegend Cat# 301805, RRID:AB_314187).

Renal cell carcinoma patient-derived organoid culturing

Frozen disassociated cells were grown in DMEM/F12 media in 30% Matrigel (Corning, Cat# 354230) on ultralow attachment plates (ULA Corning, Cat# 3473). Cells were split and washed with gentle cell disassociation media (Stemcell, Cat# 07174) and 10,000 cells mixed with 30% Matrigel and grown for 1 week before the experiment. DMEM/F12 media was supplemented with 5% FBS, 8,4 ng/mL of cholera toxin (Sigma, Cat# C8052), 0.4 µg/mL hydrocortisone (Sigma, Cat# H4001), 10 ng/mL epidermal growth factor (Corning, Cat# 354052), 24 µg/mL Adenine (Sigma, Cat# A8626), 5 µg/mL insulin (Sigma, 91077C) and 10 µM of Y-27632 RHO inhibitor (Sigma, Cat# SCM075).

Immunofluorescence and flow-cytometry on renal cell carcinoma patient-derived organoids

Gentle cell disassociation media was used on organoid cultures, and cells washed and carefully pipetted to disassociate cells. Cells were plated on 8 well Nunc; Lab-Tek; II Chamber Slides and cultured for 4 days. Cells were fixed in 4% cold paraformaldehyde and stained with CAIX (Novus Cat# NBP1-51691, RRID:AB_11011250), Vimentin (2D1) (Novus, Cat# 92 687AF647), or Cytokeratin pan (AE-1/AE-3) (Novus Cat# NBP2-33200AF750, RRID:AB_2868569) or Alexa Fluor 633 Phalloidin (Invitrogen, Cat# A22284) Microscopy pictures were taking using an EVOS FL cell imaging system (Thermo Fisher Scientific).

Ad-RFP infection and PBMC co-culture with renal cell carcinoma patient-derived organoids

A total of 100,000 VPs of Ad5-RFP were added on top of the media of already cultured organoids and RFP expression was then monitored. Cell viability of PDOs was monitored by adding 1 µM of Calcein AM (Thermo Fisher Scientific, Cat# C1430).

As for coculturing, a total of 15,000 isolated PBMCs were first stained with 1 µM Calcein AM and added on top of the media of RCC PDOs and cultured for 4 hours at 37°C. PBMC invasion was then visualized using the EVOS FL cell imaging system

Antibody-dependent cell cytotoxicity assays with renal cell carcinoma patient-derived organoid

RCC PDOs were infected with viruses at 10 or 100 MOI by adding it on top of the supernatant media and incubated for 72 hours at 37°C. PBMCs and PMNs were then added individually or combined at 100:1 and 40:1 (E:T), respectively. The number of cells in the organoids were assumed to be 10,000. After 4 hours of incubation at 37°C, cell killing was measured by determining the amount of LDH released using a colometric assay (CyQUANT LDH Cytotoxicity Assay, Cat# C20303). Specific lysis was then calculated as stated before.

Statistical analysis

Statistical analysis was performed using GraphPad Prism 7 (GraphPad Software, La Jolla, California, USA). Data were analyzed using an unpaired t-test where n≥3. Levels of significance were set at *p<0.05, **p<0.01, ***p<0.001 and ****p<0.0001. Error bars represent SEM.

RESULTS

Characterization of an oncolytic adenovirus expressing IgGA-chimeric anti-PD1 Fc-fusion peptides

In this study, we generated an oncolytic adenovirus, Ad-Cab (Adenovirus-ChimericAntibody), expressing a chimeric IgG-IgA (IgGA) Fc linked to an enhanced PD-1 ectodomain via a glycine linker able to bind to PD-L1 (figure 1A). This was cloned in the gp19K+7.1K region of the E3A gene (figure 1B) and with an MTS cell viability assay, we could show that the genetic modification did not affect the oncolytic fitness or replication of the virus (online supplemental figure S1A).

First, the Fc-fusion peptide production was tested by western blot analysis. Ad-Cab was able to secrete a 100 kDa Fc-fusion peptide, under native conditions, in the supernatant of A549 cells at 48 hours after incubation (online supplemental figure S1B). As expected, the Fc-fusion peptide comprised of a homodimer connected via a sulfide bridge, since a 50 kDa band was observed under denaturing conditions (online supplemental figure S1B). Next, we assessed the amount of Fc-fusion peptide secreted at different time points of infection. After 1 day of infection in A549 cells, Ad-Cab secreted approximately 2 µg of the Fc-fusion peptide and production kept increasing till day 3 reaching 7 µg (figure 1C). To assess whether the produced Fc-fusion peptide could bind to PD-L1, we performed a competition assay with a commercially available anti-PD-L1 (Atezolizumab), a well-established binder of PD-L1 and disruptor of the PD-1/L1 axis. To this end, we coincubated A549 cells with increasing concentrations of Fc-fusion peptides, purified from the supernatant of infected cells, followed by the addition of 10 µg/mL of Atezolizumab. Detection of bound Atezolizumab to PD-L1 was then analyzed by adding a secondary PE labeled antihuman IgG not able to recognize the Fc-fusion peptide. When no Fc-fusion peptide was added Atezolizumab was able to bind to PD-L1 (figure 1D). Yet, as the concentration

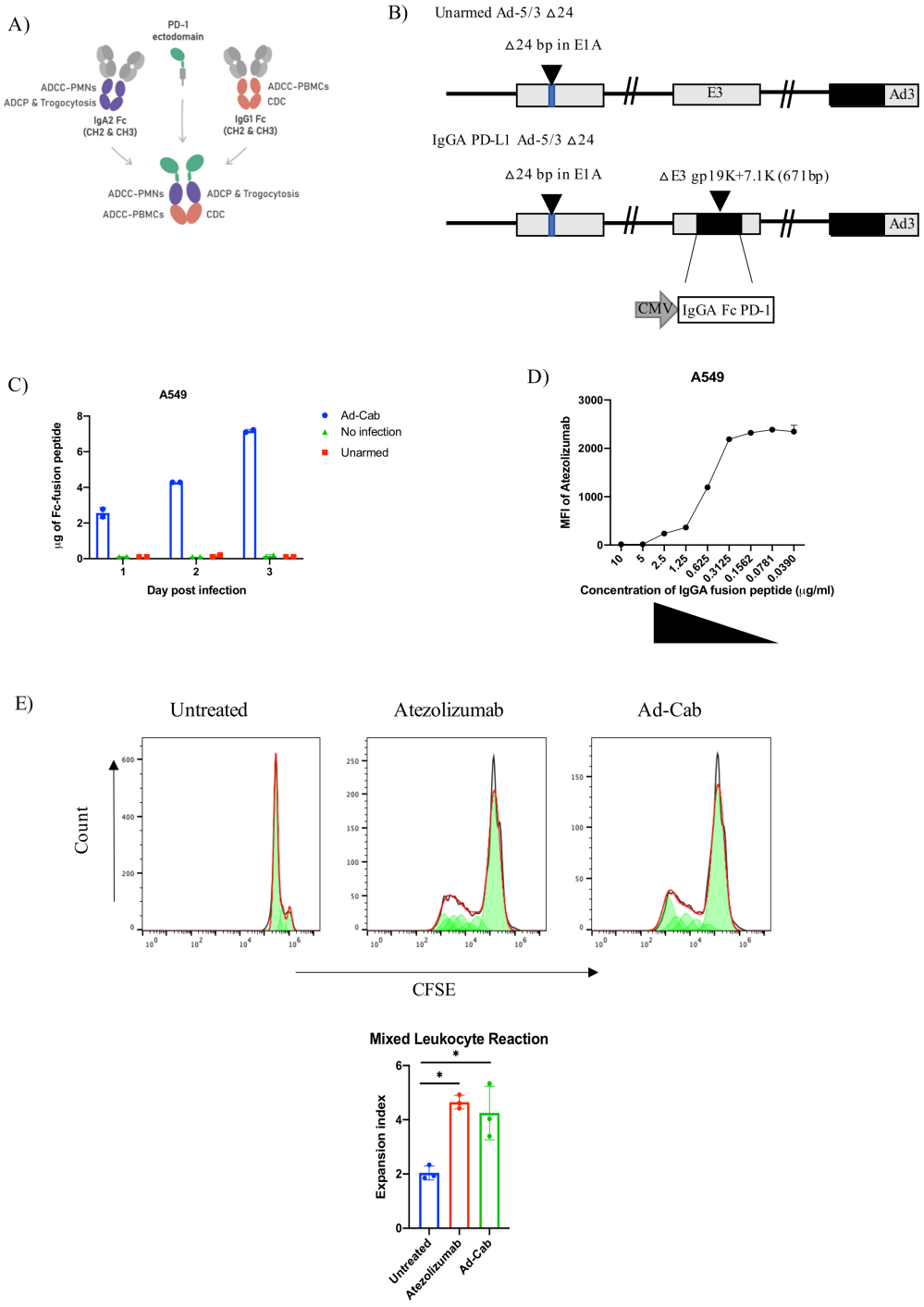

Figure 1 Characterization of Ad-Cab. (A) Graphical representation of the IgGA Fc-fusion protein; the cross-isotype Fc is made up of the CH chains 2 and 3 of an IgA2 (purple) and IgG1 (orange) attached to an PD-1 ectodomain (green) via a glycine linker. The IgGA Fc employs effector mechanism of both an IgG1 and IgA2. (B) Schematic representation of oncolytic adenovirus 5/3 delta 24 (Ad5/3 Δ24) constructs with modifications in the E1, E3 and fiber regions. Black inverted triangles represent deletions. Both unarmed Ad5/3 Δ24 (Unarmed) and IgGA PD-L1 Ad-5/3 ▵24 (Ad-Cab) have a 24 base-pair deletion in the E1 region, leading to conditionally replicate in Rb-deficient cells, and a serotype 5 fiber knob with serotype 3 knob. The IgGA PD-L1 fusion protein cassette consisted of CMV promoter and enhancer and was cloned into the gp19k+71 .k region. (C) Quantification of IgGA Fc-fusion proteins over time. A549 cells were infected with 100 MOI of Ad-Cab and Unarmed virus and supernatants were collected at different indicated time points. IgGA Fc-fusion proteins were purified, and concentration was assessed by measuring absorbance at 280 nm. (D) Competitive assay between Atezolizumab and Ad-Cab. A549 cells were incubated with different concentrations of purified IgGA Fc-fusion proteins from Ad-Cab and followed by addition of 10 µg/mL Atezolizumab. Atezolizumab binding was then analyzed using an PE-labeled antihuman IgG not recognizing IgGA Fc-fusion proteins. (E) Coincubation of monocyte-derived dendritic cells with allogenic CFSE stained T cells, at a 1:10 ratio, in the presence of 1 µg/mL of Atezolizumab or isolated IgGA Fc-fusion peptide. CFSE was then measure from CD3 + CD+ 8 T cells and the expansion index was calculated. CH, constant heavy; CMV, cytomegalovirus.

of the Fc-fusion peptide increased, Atezolizumab binding decreased substantially (figure 1D). Moreover, to further demonstrate PD-L1 binding, we conducted live cell imaging to observe whether the Fc-fusion peptide could mediate close cell-contacts when PBMC were coincubated with lung carcinoma A549 cells. When Ad-Cab (online supplemental movie S1) was added, PBMCs were shown to be in clear proximity to A549 compared with when we added Atezolizumab, a clinical PD-L1 antibody holding a N298A mutation abrogating Fc-binding (online supplemental movie S2). To test the ability for the Fc-fusion peptide to activate CD8 + T cells, an allogenic mixed leukocyte reaction was performed. In this assay, monocytic-differentiated dendritic cells from one donor were mixed with isolated CFSE stained PBMCs from another donor to mimic the immunosuppressive effects of PD-L1/PD1 interactions. Samples were treated with or without Atezolizumab or purified IgGA Fc-fusion peptide to test whether the blocking of PD-L1 could induce a T cells expansion (figure 1E). When Atezolizumab and IgGA Fc-fusion peptide were added, a clear expansion of CD8 + T cells was observed, correlating with a decrease in CFSE compared with untreated. When calculating their expansion index, both Atezolizumab and IgGA Fc-fusion peptide were higher than the mock. Taken together, we demonstrated that Ad-Cab can secrete high levels of Fc-fusion peptide that is able to bind to PD-L1, outcompete Atezolizumab and activate CD8 + T cells.

The secreted Fc-fusion peptides activate effector mechanisms of an IgG1 and an IgA1

After testing expression and binding, we examined the ability of the Fc-fusion peptides to activate antibody effector mechanisms. Since the Fc entails a hybrid of an IgG1 and an IgA1, CDC and ADCC were tested with both PMN and PBMCs on six different human and murine tumor cell lines expressing varying levels of PD-L1 (figure 2A). Murine breast cancer (4T1), murine colon carcinoma (CT26) and murine melanoma cell lines (B16F10 and B16F1) were used since oncolytic human adenoviruses cannot induce oncolysis and cytotoxicity in most murine cell lines and thus the effects seen can then be attributed to the Fc-activation of effector mechanisms. Cells were first infected with either Ad-Cab or unarmed oncolytic adenovirus (Ad-5/3 Δ24) at two different MOIs (10 and 100) for 2 days to limit oncolysis with human cell lines (MDA-MB-436 and A549). Subsequently, when complement active serum was added, cell lysis could be observed with Ad-Cab infected cells (figure 2B). Already at MOI 10, cell lysis was occurring and was further augmented as the MOI increased to 100 in all six cell lines. As expected, cell lysis was not shown with the control virus (Ad5/3-delta 24) in all conditions, further attributing cell death to CDC induction, especially in the human cell lines where viral oncolysis can be induced.

ADCC assays were then tested with two different immune populations: PBMCs (figure 2C) and PMNs (figure 2D). In contrast to CDC, at MOI 10 minimal or no induction of ADCC could be seen with all cell lines infected with Ad-Cab when PBMCs or PMNs were added. Nevertheless, when the MOI increased to 100, cell lysis was observed with both populations. Interestingly, both PMNs and PBMCs were able to elicit similar levels of cytotoxicity with all the cells.

Finally, we wanted to test the ability of Ad-Cab to activate macrophages and induce ADCP. The ability to elicit ADCP was determined by the uptake of CFSE by macrophages from the tumor cell lines labeled with CFSE. At MOI 10, no uptake of CFSE was observed with any condition yet at MOI 100, an increase of CFSE uptake by the macrophages could be observed in all cell lines when Ad-Cab was added (figure 2E). Overall, the data demonstrate that the secreted Fc-fusion peptide can induce the effector mechanisms of both an IgG1 and an IgA.

Trogocytosis drives the PMN-mediated ADCC

It has been previously shown that in order to initiate ADCC in vitro, PMNs adhere to the target cells establishing an immunological synapse with the antibody-opsonized tumor cells.[27] This subsequently causes the disruption of their plasma membrane and the endocytosis of cytoplasmic fragments, leading to a necrotic type of cell death termed trogocytosis. In order to explore the possible nature of the cytotoxic mechanism during PMN-mediated ADCC, we quantified the transfer of membrane from tumor cells to PMNs by flow cytometry. Virally infected cells had their lipid membrane labeled with 3,30-dioctadecyloxacarbocyanine perchlorate (DiO), after which unstained neutrophils were added to the cell culture. Neutrophils were first gated using the side and forward scatter since they are smaller than a tumor cell and also confirmed with neutrophil markers such as CD15 + and CD14− (online supplemental figure S2). The MFI of DiO was then measured on these neutrophils after incubation in three different conditions: without exposure to the target cells (figure 3A), with exposure to uninfected stained cells (figure 3B) and with exposure to Ad-Cab infected stained cells (figure 3C). When neutrophils were examined on their own, without former exposure to the target cells or when they were added to uninfected stained tumor cells, there was no DiO measured, and no membrane transfer had happened. Yet, when the neutrophils were added to Ad-Cab infected cells, an uptake of DiO was observed by PMNs. This implies the uptake of the lipid membrane of the infected tumor cells by the neutrophils, which is a characteristic of trogocytosis. The same procedure was performed using all six cell lines and an increase in DiO MFI in the neutrophils was noted only when neutrophils had previously been exposed to cancer cells infected with the Ad-Cab and not with the other controls used (figure 3D). Hence, these findings add evidence in support that one of the mechanisms in which PMNs employ ADCC with Ad-Cab is trogocytosis.

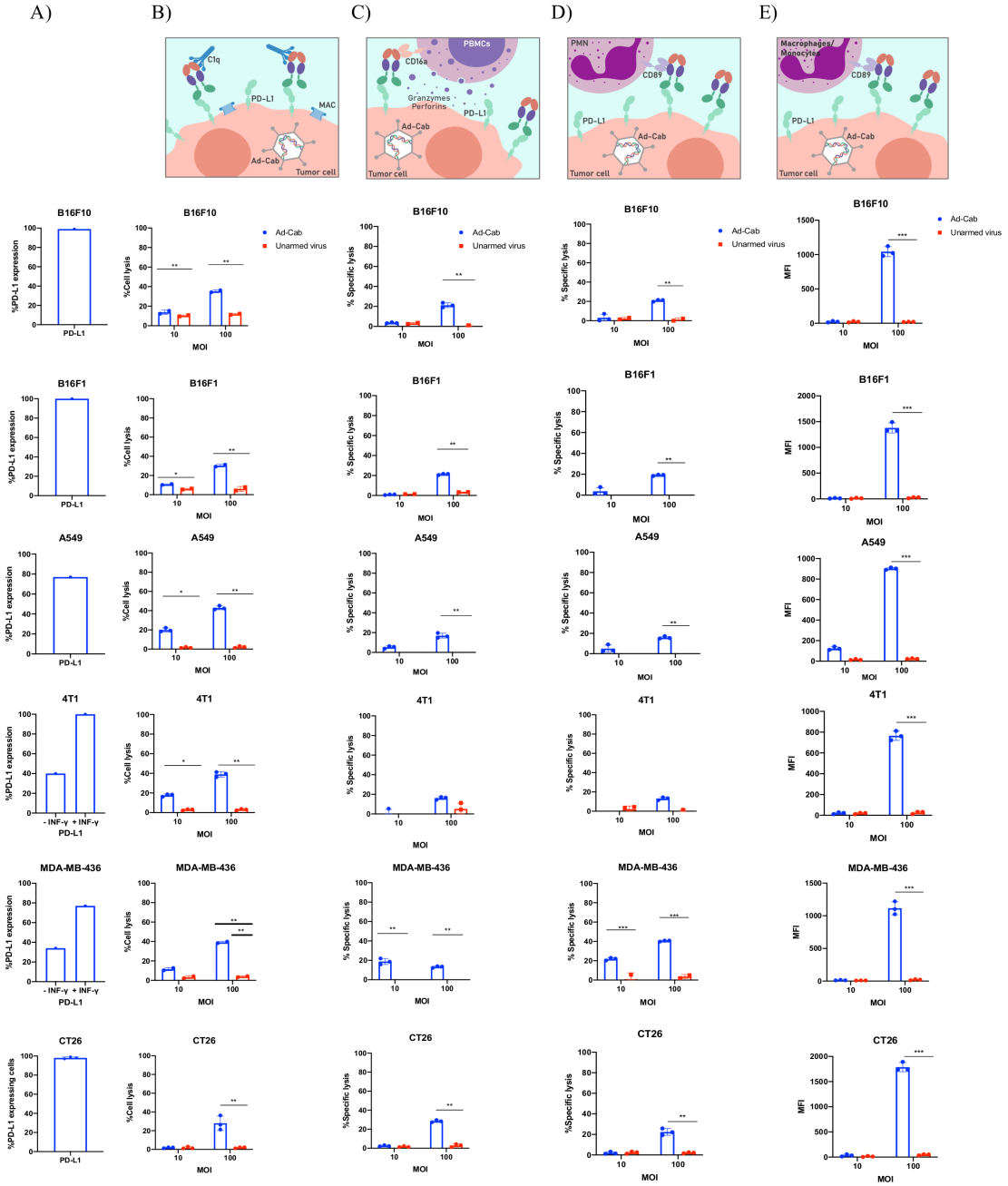

Figure 2 Activation of multiple branches of the immune system. (A) The percentage of PD-L1 expression on all cell lines used in the assays. (B) FACS-based CDC assay against all six different cell lines with Ad-Cab and Unarmed virus. Cells were infected at two indicated MOIs, incubated for 48 hours and pooled serum from healthy volunteers was then added at a final concentration of 15.5%. After 4 hours at 37°C, cell lysis was measured using 7-AAD. ADCC against five different cell lines using either (C) PBMCs or (D) PMN as effector cells. Indicated viruses were added at 10 and 100 MOI and incubated for 48 hours. Subsequently, PBMCs and PMNs were added at an E:T ratio of 100:1 and 40:1, respectively, and lysis was by quantifying LDH release after 4 hours at 37°C. (E) ADCP was measured by incubating target cells with 10 or 100 MOI of Ad-Cab or unarmed virus for 48 hours. Then, cells were labeled with CFSE and macrophages were added at a 5:1 (effector:target) ratio. Phagocytosis was quantified by measuring the uptake of CFSE by macrophages. Levels of significance were set at *p<0.05, **p<0.01, ***p<0.001 and ****p<0.0001. Error bars represent SD. AAD; amino-actinomycin D; ADCC, antibody-dependent cell cytotoxicity; ADCP, antibody-dependent cell phagocytosis; CDC; complement-dependent cytotoxicity; PBMC; peripheral blood mononuclear cell; PMN, polymorphonuclear.

Ad-Cab induces higher tumor cytotoxicity with multiple immune populations while leaving myeloid cells untouched

We hypothesized that a synchronous activation of the multiple branches of the immune system would lead to enhanced tumor cell killing and complete clearance of the tumor. To test this, we again performed the ADCC assays with different combinations of immune components such as PBMCs+PMNs or PBMCs+PMNS+serum with the same cell lines as previously expressing PD-L1 (figure 4A). Also, to further examine this, we used Atezolizumab, which

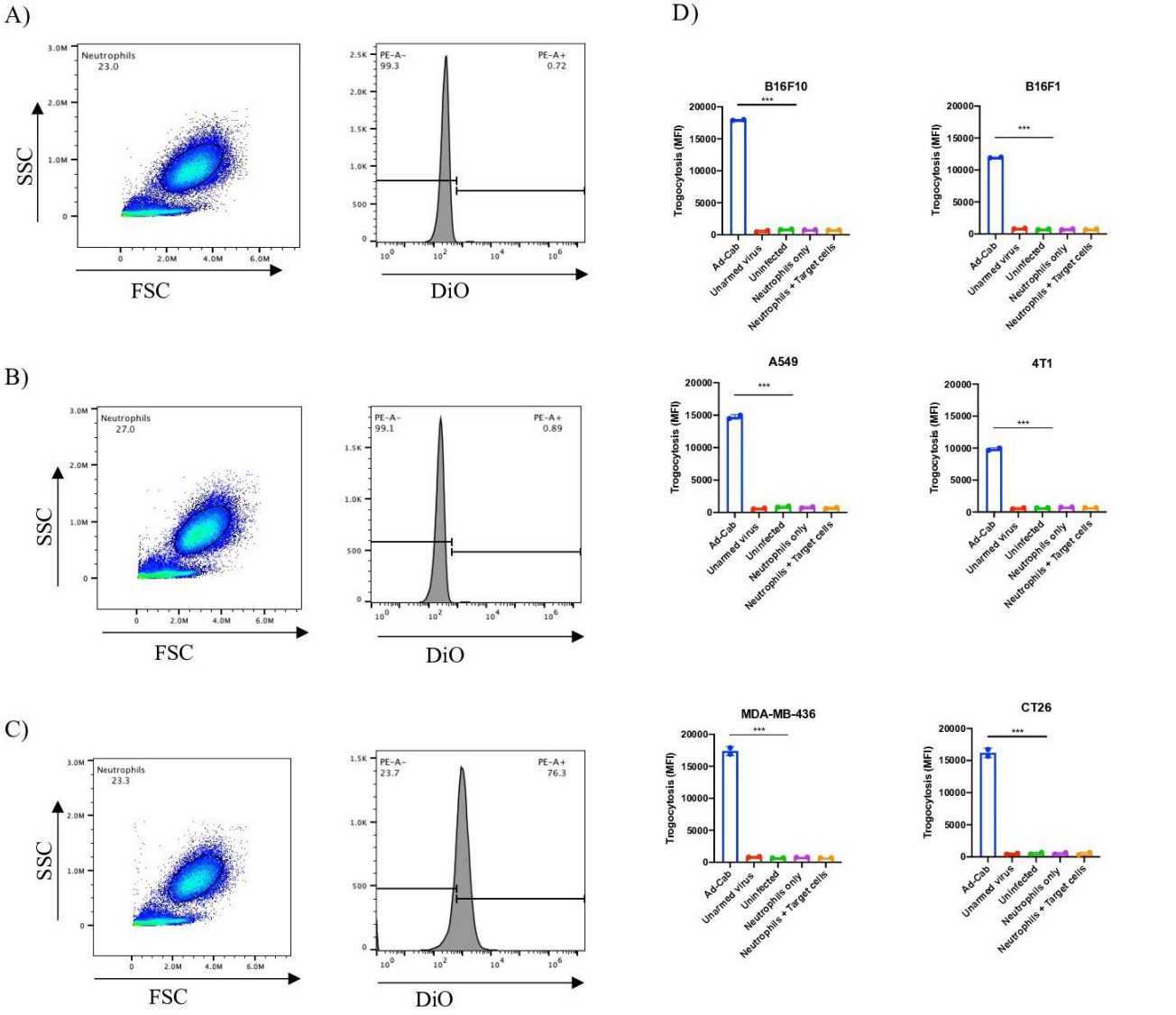

Figure 3 PMN's mode of action during ADCC. Gating strategy (left) and histogram (right) of neutrophils incubated alone (A), with DiO stained A549 cells (B) or DiO stained A549 cells infected with 100 MOI of Ad-Cab (C). Trogocytosis of six different cells lines infected at 100 MOI (D) for 48 hours with indicated virus and PMNs added. Neutrophils alone or neutrophils coincubated with DiO stained target cells were used as controls. PMNs were added at an E:T ratio of 40:1. DiO +PMNs were then calculated using flow cytometry. ADCC, antibody-dependent cell phagocytosis; PMN, polymorphonuclear.

holds a N298A mutation abrogating its effector mechanisms, Atezolizumab without the mutation, designated IgG1-PD-L1, able to elicit effector mechanisms of an IgG1 and an IgA-PD-L1. When each immune component was added individually (online supplemental figure S3B–D), Atezolizumab carrying the N298A mutation was not able to induce cell lysis. Interestingly, the functional IgG1 PD-L1 antibody was able to induce similar cell lysis levels as the Fc-fusion peptides when the complement system or PBMCs were added. Nevertheless, the IgG1 PD-L1 was able to induce only minimal cell lysis with PMNs compared with the Fc-fusion peptides. As expected, IgA-PD-L1 was only able to activate PMNs and not PBMCs or the complement system.

When PBMCs and PMNs were added together, a significant cytotoxicity augmentation, compared with the cell populations alone, was observed with Ad-Cab (figure 4B). This was not seen with IgG1- or IgA-PD-L1 where cell lysis levels remained like when PBMCs or PMNs were added alone, respectively. Meanwhile, when all three components (fresh human serum, PBMCs and PMNs) were added together, enhanced cytotoxicity could again be noticed with Ad-Cab and IgG1-PD L1 (figure 4C). Interestingly, IgG1 PD-L1 showed a significant increase in cell lysis compared with when serum or PBMCs were added together. This again further reinforced the added benefit of activating multiple immune branches. Moreover, the addition of serum to the combination of PBMCs+PMNs also significantly increased cell lysis with Ad-Cab. This increase in cell lysis almost reached full clearance of PD-L1 expressing cells. Notably, this synergistic effect was demonstrated with B16F10, B16F1 and

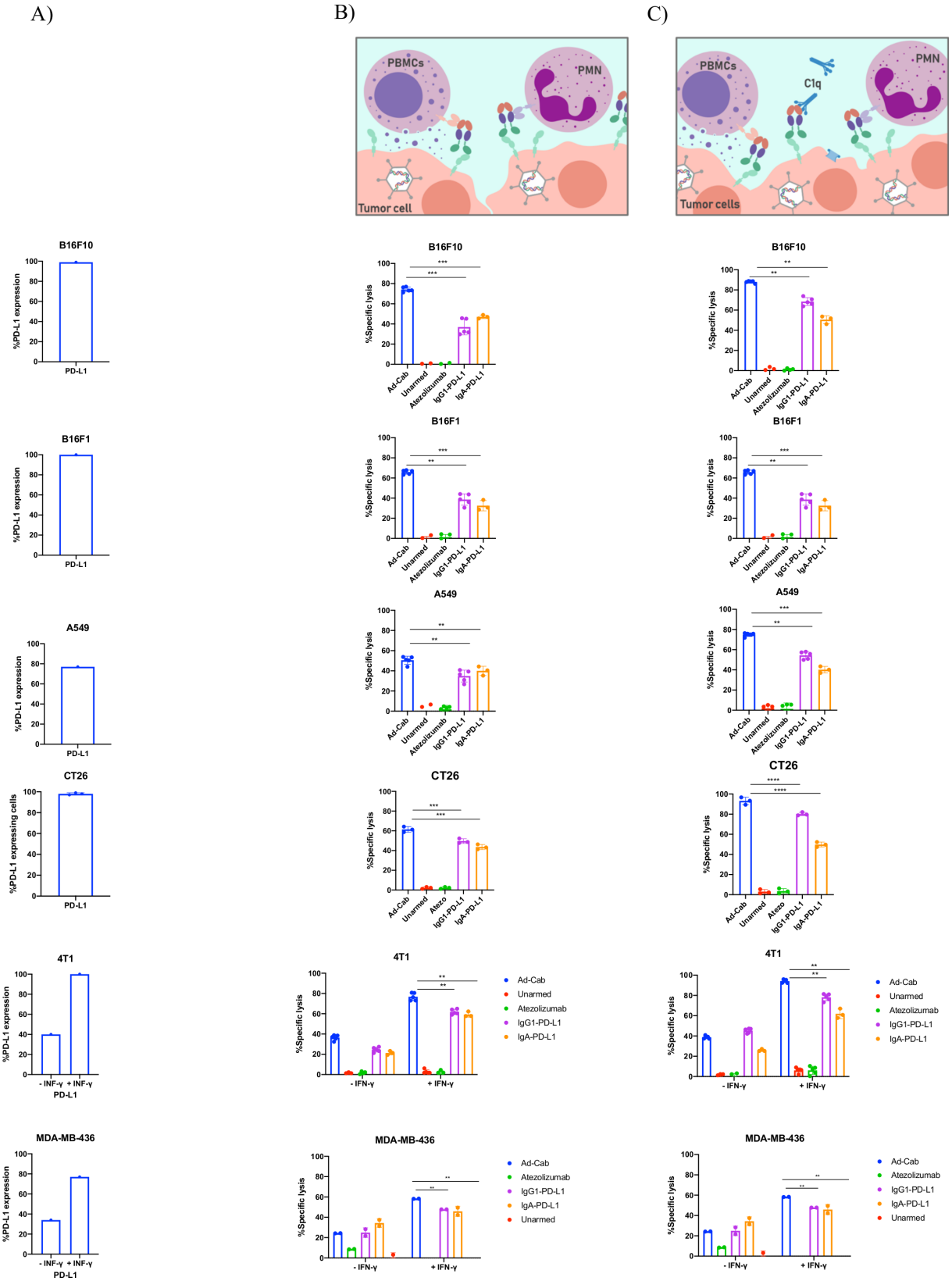

Figure 4 Activation of multiple branches works in synergy leading to enhanced cytotoxicity. (A) Histograms demonstrating the percentage PD-L1 expression on all cell lines used in the assays. Cell lysis of tumor cell lines in the presence of (B) PBMCs +PMNs and (C) PBMCs+PMNs+serum . PBMCs and PMNs were added at an E:T ratio of 40:1 and 100:1, respectively, while serum was added at 15.5%. Cells were infected with viruses at 100 MOI and incubated for 48 hours or 10 µg/mL of antibody were added 30 min prior to adding immune components. Lysis was then detected using an LDH release assay. Levels of significance were set at *p<0.05, **p<0.01, ***p<0.001 and ****p<0.0001. Error bars represent SD. PBMC; peripheral blood mononuclear cell; PMN, polymorphonuclear.

A549 cells but not with 4T1 and MDA-MB-436 cells. We speculated that this was because most of the PD-L1 expressing 4T1 and MDA-MB-436 cells had already been eliminated when each component of the immune system was added individually. To examine this, PD-L1 expression on 4T1 and MDA-MB-436 cells was further increased by treating cells overnight with IFN-gamma before setting the ADCC assays.[28] As anticipated, a higher tumor killing could be observed with all immune components added individually or in combination with IFN-gamma treated 4T1 and MDA-MB-436 cells. Like the other cell lines, with the IFN-gamma treated cells, Ad-Cab was able to activate PMNs and induce higher killing with both combinations (PBMC+PMN and PBMCs+PMNs+serum) compared with IgG1 PD-L1.

To further verify such data, we performed both live-cell microscopy and impedance-based real-time quantitative analysis (XCELLigence) to track target cells treated with purified Fc-fusion peptide (Ad-Cab) or therapeutic antibodies (Atezolizumab and IgG1-PDL1) following the addition of PBMCs and PMNs. With live-cell microscopy, A549 cells were monitored for 12 hours, and death was determined using a Caspase-3/7 Green Reagent and phase confluency. At E:T ratios of 10:1 and 4:1, PBMCs and PMNs, respectively, live-cell imaging supported the LDH release data since apoptosis was observed when IgG1-PD-L1 or Ad-Cab was added (online supplemental figure S4A and online supplemental movie S3-5). Moreover, cell death was further enhanced with Ad-Cab compared with IgG1-PDL1 (online supplemental file 4). Using XCELLigence, we analyzed cell-killing in real time (online supplemental figure S5A–E) and calculated the rate of cell death for each therapeutic antibody (IgG1- or IgA-PD-L1) and purified Fc-fusion peptide. The purified Fc-fusion peptide (Ad-Cab) had the highest killing rate in all cell lines, ranging from 0.0361 to 0.0482, compared with IgG-PD-L1 (0.0221–0.0289) and IgA-PD-L1 (–0.0186 to 0.0282) (online supplemental figure S5F). Hence, we demonstrated that the Fc-fusion peptide augment immune-mediated apoptosis compared with IgG1-PD-L1, IgA-PD-L1 and the clinically used Atezolizumab in real time analysis.

Other than cancer cells, immune cells also express PD-L1, especially myeloid cells. To test whether Ad-Cab could affect such cells, purified IgGA Fc fusion peptide was added in unprocessed whole blood of three healthy donors and incubated for 24 hours. In these conditions, we would be able to test whether the Fc-fusion peptide could induce lysis of any immune population in the presence of all physiological effector populations (NK cells, neutrophils or complement system). After 24 hours, samples were processed and stained, and counting beads were added to determine the absolute numbers of DCs, NK cells, neutrophils, T cells and monocytes (online supplemental figure S6A). Ad-Cab was shown not to induce cytotoxicity to any cell population since the percentages and absolute numbers were similar to untreated or Trastuzumab (anti Her-2 IgG) treated samples in all three donors (online supplemental figure S6B).

In vivo efficacy of Ad-Cab with CT26 and A549 tumor model

Based on the in vitro data, we decided to test the efficacy of Ad-Cab in vivo using a syngeneic mice model. Mice do not express Fc-α receptors, hence not allowing to test the full efficacy of the Fc-fusion peptide. Nevertheless, due to the homology of human and murine Fc-γ receptors, the IgG portion of the Fc-fusion can be tested. The colon carcinoma CT26 model was used since it has been reported not to respond effectively to PD-L1 checkpoint therapy and the advantages of Ad-Cab could be more apparent in this model.[29 30] After 7 days postengraftment, mice were treated either with PBS, Ad-5/3Δ24, Ad-Cab or mPD-L1 for a total of 7 times (figure 5A). As expected, Ad-Cab was shown to be the most effective group in controlling tumor growth (figure 5B). Also, mice treated with mPD-L1 were shown to control tumor growth better than mock; however, this was not statistically significant. We also calculated a therapeutic threshold based on the average of the tumor growth of mice treated with Ad-5/3-Δ24 and mPD-L1 since Ad-Cab represents a combination of both treatments. Based on this, all the mice treated with Ad-Cab were responders showing a superior efficacy compared with mPD-L1 (online supplemental figure S7A). The efficacy of Ad-Cab could also be translated to an enhanced overall survival compared with all the other treatment groups (figure 5C). Due to toxicity concerns, we analyzed the weight of the mice and distribution of the antibody for each group. No significant weight changes could be seen among the groups (online supplemental figure S7B). Moreover, because the Fc fusion peptide was tagged with an 8xHis, we monitored the distribution in the blood and tumor. After the mice had received four treatments, two mice from each group were sacrificed and their blood and tumors were collected to detect the Fc-fusion peptide. In blood (figure 5D), undetectable levels of his-tagged Fc-fusion peptide could be observed in all groups. However, in the tumor (figure 5E), only in the Ad-Cab group an average of 2 µg/mL of his-tagged Fc-Fusion peptide could be found. After observing that from the Ad-Cab and mPD-L1 treated groups, some mice were tumor free, we decided to rechallenge the mice with CT26 to assess if a memory response had been formed. Mice previously treated with mPD-L1 had a successful tumor implantation, yet the growth was reduced compared with naïve mice injected with CT26 (figure 5F). Interestingly, mice treated with Ad-Cab rejected the tumor since no tumor was visible up to 30 days. This indicated that the surviving mice from the Ad-Cab group had formed a memory response able to control a rechallenge of CT26.

We went on to further characterize Ad-Cab in a human tumor xenograft model with immune deficient NS (NOD/SCID) mice reconstituted with a human immune system. NS mice were first implanted with A549 cells and also injected with freshly isolated PBMCs from the same donor (figure 5G). After tumors had been

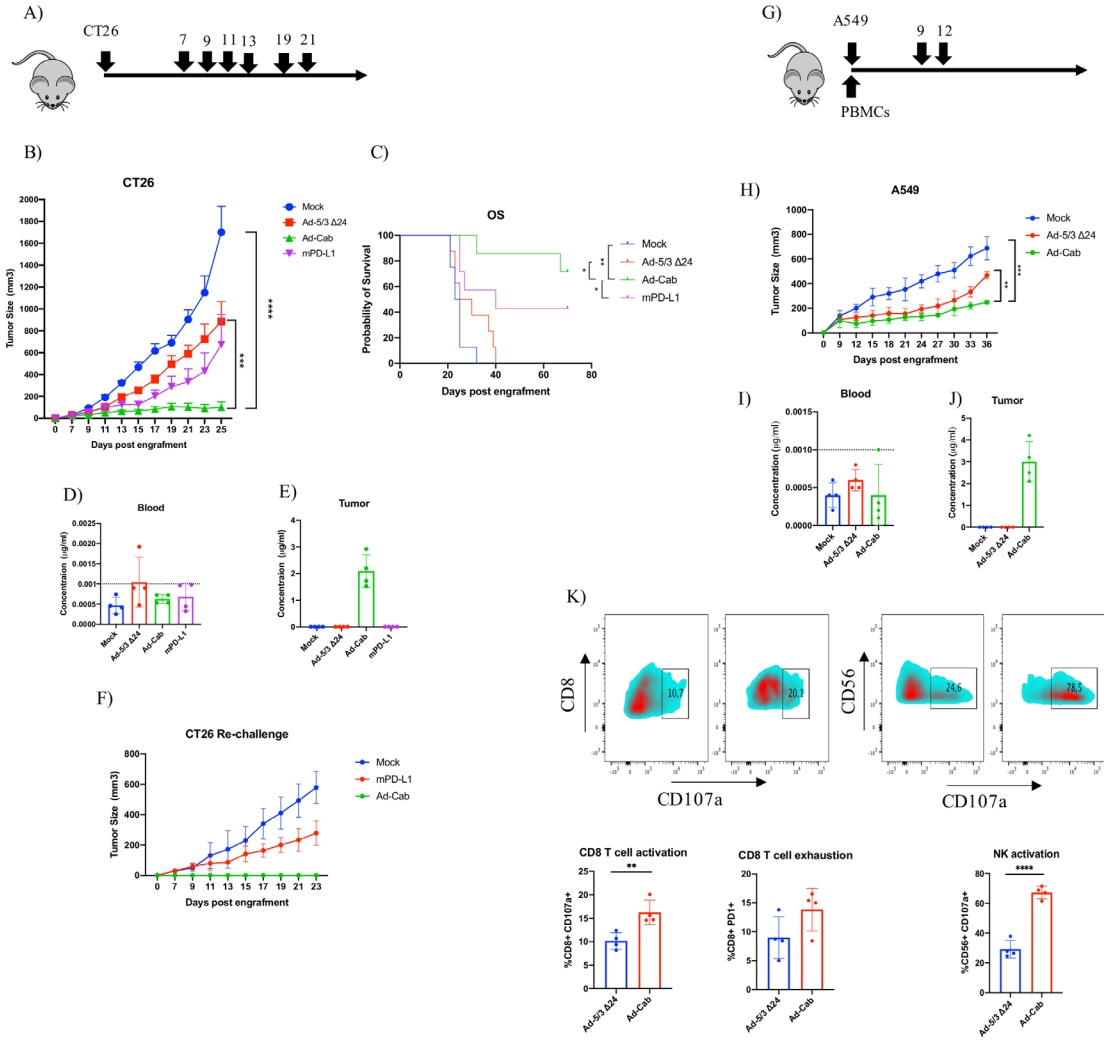

Figure 5 Tumor efficacy and biodistribution of Ad-Cab in syngeneic mouse model CT26 colon carcinoma and xenograft model A549. (A) Schematic diagram of treatment schedule. Mice were treated either with PBS (mock), Ad-5/3Δ24, Ad-Cab or mPD-L1 after 7 days postengraftment of 5×10^6 cells in the right flank of the mice. Treatments were given on days 7, 9, 11, 13,17, 19 and 21. Ad-5/3Δ24 and Ad-Cab were given intratumorally at a dose of 1×10^9 viral particles while 100 µg of mPD-L1 was given intraperitoneally. (B) Summary data for average tumor growth for all treatment groups for CT26 tumor model. (C) Kaplan-Meier survival curve for the treatment groups. Concentration of His-tagged PD-L1 Fc-fusion peptide in blood (D) and tumor (E) from two mice per each group. Dotted line represents the detection limit of the kit. (F) CT26 tumor free mice were rechallenged with 500,000 CT26 cells and tumor growth was recorded. (G) Schematic diagram of treatment schedule A549 model. Mice were implanted with tumors and human PBMCs and then treated with PBS (mock), Ad-5/3Δ24 or Ad-Cab. Treatments were given on days 9 and 12 at a dose of 1×10^9 viral particles intratumorally.(H) Summary data for average tumor growth for all treatments with A549 bearing mice. Concentration of His-tagged PD-L1 Fc-fusion peptide in blood (I) and tumor (J) from two mice per each group. (K) CD8 + T cell and NK cell degranulation (CD107a) and exhaustion (PD-1) markers were examined in the tumor microenvironment. A two-way ANOVA was conducted along with a Dunnett's test to test significance. The number of mice per each group was 9–10. Levels of significance were set at *p<0.05, **p<0.01, ***p<0.001 and ****p<0.0001. Error bars represent SD. ANOVA, analysis of variance; NK, natural killer; PBMC; peripheral blood mononuclear cell.

engrafted, peripheral blood was taken from the mice to check for human immune cells engraftment. It was seen that human CD45 and CD3 cells were circulating in the peripheral blood of the mice, suggesting that the engraftment with human PBMCs was successful (online supplemental figure S8). Mice were treated with either PBS, Ad-5/3 Δ24 or Ad-Cab for two treatments. Mice treated with unarmed oncolytic adenovirus had a better tumor control compared with mock (figure 5H). Yet, mice treated with Ad-Cab had a statistically significant tumor control compared with all other groups. Similar with the CT26 mice, his-tagged Fc-fusion peptide was not found in the blood (figure 5I) in any group but in the tumors of Ad-Cab treated mice around 2–4 µg of his-tagged protein was observed (figure 5J). By analyzing the tumor microenvironment, we observed that mice treated with Ad-Cab had an increase in both NK and CD8 + T cells which were positive for CD107a (figure 5K). This indicated that these cells had been activated and degranulated perforins and granzymes. These data demonstrate

the enhanced in vivo efficacy and good safety profile of Ad-Cab.

Ad-Cab controls 4T1 tumor growth despite CD8+ T cell depletion

After observing that Ad-Cab was successful in controlling CT26 and A549 tumors in vivo, we decided to test it against 4T1 which is a highly immunosuppressive, fast growing and metastatic tumor. Mice bearing 4T1 tumors were treated with the same treatments and dosing as with the CT26 mice (figure 6A). Mice treated with Ad-Cab showed the best tumor control over all other groups. mPD-L1 treated mice also showed a degree of tumor control, yet it was not significant compared with mock (figure 6B). After sacrificing the mice, the tumor microenvironment was analyzed for different immune populations and activation/exhaustion markers. As expected, 4T1 tumors were highly infiltrated with both immunosuppressive monocytic (CD11b+Ly6 Chi Ly6G-) and granulocytic (CD11b+Ly6 Ghi Ly6C-) myeloid-derived suppressor cells (MDSC) which is in line with previous reports (figure 6C). Surprisingly, there was a significant reduction in both granulocytic MDSC (figure 6D) and monocytic MDSC (figure 6E) cell populations in the Ad-Cab treated group compared with other groups. Moreover, this reduction in the Ad-Cab treated group was accompanied with a higher infiltration of NK cells compared with the rest of the groups (online supplemental figure S9). No increase of other cell types such as dendritic cells, CD8 T-cells, CD4 T-cells (online supplemental figure S9) or tumor-associated macrophages (TAMs) (figure 6F) was observed since the percentage of cells was similar among all groups. We then analyzed the activation of both CD8 + T cells and NK cells using the cytotoxic degranulation marker CD107a (figure 6G). A clear increase of NK activation and degranulation could be observed in Ad-Cab treated groups (figure 6H). This was also seen with the CD8 T cells with the Ad-Cab treated group but as well with the mPD-L1 treated group (figure 6I). Other than being activated, CD8 T-cells displayed an exhausted phenotype in both Ad-Cab and mPD-L1 group with the latter being higher in expressing exhaustion marker PD1 (figure 6J). This implies that both Ad-Cab and mPD-L1 were able to activate and degranulate CD8 + T cells against the tumor but Ad-Cab was also able to do so with NK cells as well.

Having observed that Ad-Cab was able to strongly activate NK cells, we wanted to further characterize their mechanism of action in vivo by repeating the same experiment with 4T1 but depleting CD8 T cells. Mice were first given a high dose of CD8 depleting antibody before starting treatment and kept receiving the depleting antibody during the treatment schedule to make sure CD8 T cells were absent during the treatment schedule (figure 6K). After the first treatment, peripheral blood was taken from mice to check that no circulating CD8 T cells were present. Depletion was shown to be successful as no circulating CD8 T cells could be observed in mice receiving CD8 depleting antibody compared with those that were not (figure 6L). As expected, mPD-L1 treated mice showed a similar tumor growth compared with mock and Ad-5/3 Δ24 treated mice. Nevertheless, Ad-Cab treated mice had a significantly lower tumor growth compared with all other groups (figure 6M). This was also translated to higher overall survival in the Ad-Cab treated group (figure 6N). This indicates that, in contrast to checkpoint inhibitors, Ad-Cab does not solely require CD8 T cells to induce tumor killing in vivo.

Characterization of patient-derived RCC organoids as testing platforms for Ad-Cab

To further study the contribution of the IgA portion of Ad-Cab, we developed a novel testing platform using RCC PDOs. Freshly dissociated tumor tissue from four patients (RCC1-4) undergoing radical nephrectomies were obtained. Samples were grown either as 2D in 3D by embedding cells in Matrigel (figure 7A). In order to assess the heterogeneity of the PDOs and to compare them to the corresponding tumor tissue that they originated from, we stained PDO cells that were allowed to grow as 2D on plastic with three commonly used stains to differentiate RCC (CAIX, Vimentin and Cytokeratin) and with an F-actin stain (Phalloidin) (figure 7B). Both CAIX and vimentin are highly sensitive and specific for clear cell renal cell carcinoma (ccRCC).[31] This is consistent with the staining since RCC2, RCC3 and RCC4 samples were shown to be positive for CAIX and vimentin and were characterized as ccRCC at the time of diagnosis. Surprisingly, RCC1 was both CAIX and vimentin positive despite being classified as a chromophobe RCC, a subtype that usually is not CAIX or vimentin positive. Yet, RCC1 had a focal expression of CAIX and lower expression of vimentin compared with the other samples, where staining was more diffused.

Subsequently, we tested whether oncolytic adenoviruses had the ability to pass through the Matrigel and infect the organoids. To this end, we infected PDOs with an oncolytic adenovirus expressing the red fluorescent protein (Ad5-Δ 24-RFP) to visualize the infection and the replication of the virus (figure 7C, online supplemental figure S10A–C). The virus was added on top of the supernatant of the PDO cultures and after 1 day PDOs were already infected and expressing RFP. Expression kept increasing until reaching a maximum on day 3. To confirm whether the virus could induce oncolysis, a viability cell stain, Calcein AM, was added and monitored (figure 7C). Oncolysis was observed to start at day 3 with minimal death occurring, and by day 4, most cells were shown to be dead. To finalize the testing platform, we tested whether isolated PBMCs could travel through the Matrigel and surround the organoids. Before their addition to the organoid cultures, PBMCs were labeled with Calcien green and then added on top of the media (figure 7D). Within hours, they could be seen to pass through the Matrigel and surround organoids. Finally, PD-L1 expression was then tested by dissociating the PDOs into single cells and evaluating expression using flow cytometry (figure 7E).

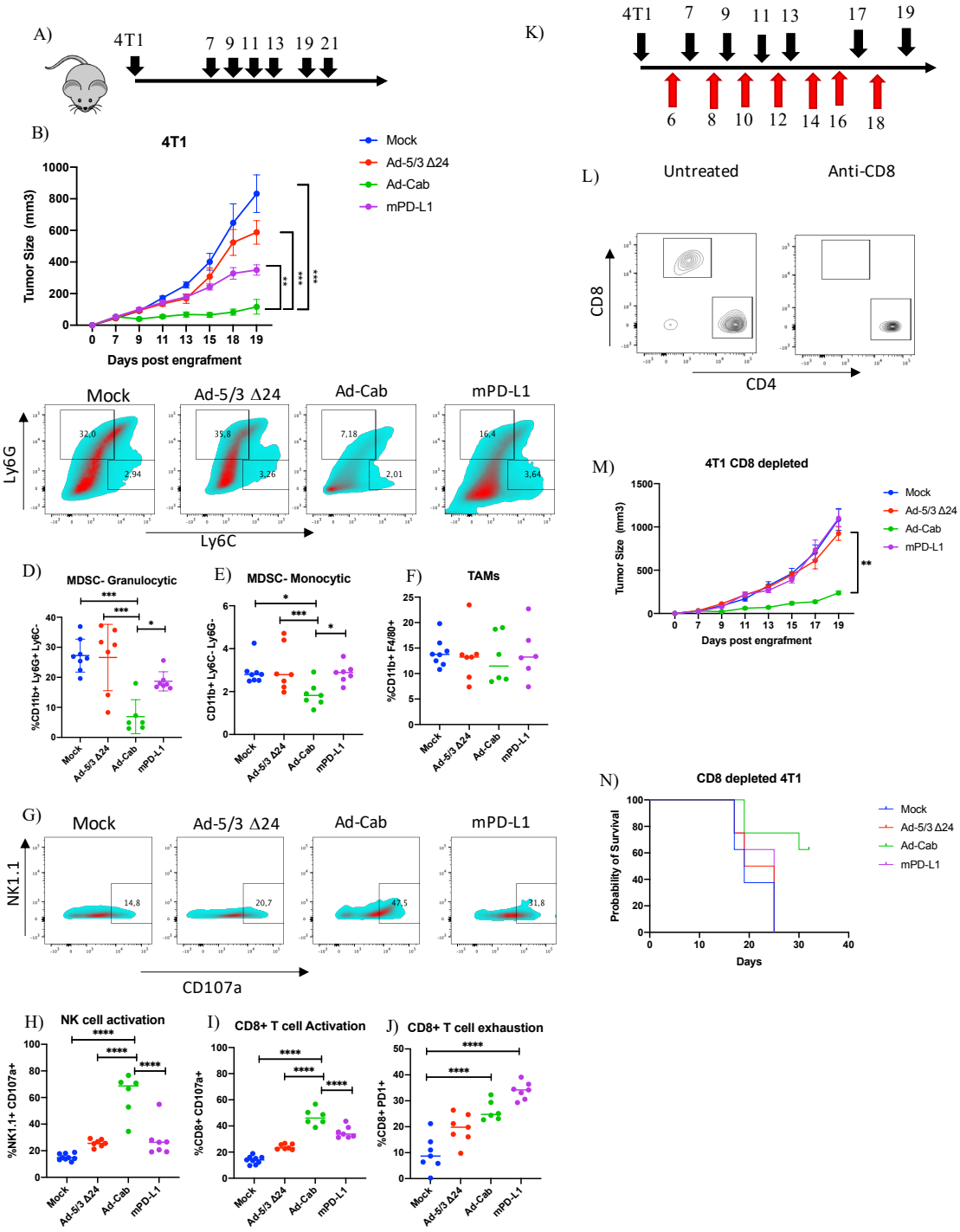

Figure 6 Ad-Cab induces 4T1 tumor control in vivo in presence and absence of CD8 + T cells. (A) Schematic diagram of treatment schedule for 4T1 bearing mice. Mice were treated either with PBS (mock), Ad-5/3Δ24, Ad-Cab or mPD-L1 after 7 days postengraftment of 3×10^5 cells in the right flank of the mice. Treatments were given on days 7, 9, 11, 13,17, 19 and 21. Ad-5/3Δ24 and Ad-Cab were given intratumorally at a dose of 1×10^9 viral particles while 100 µg of mPD-L1 was given intraperitoneally. (B) Summary data for average tumor growth for all treatment groups for 4T1 tumor model. (C) Granulocytic (CD11b+Ly6 Ghi Ly6C-) and monocytic (CD11b+Ly6 Chi Ly6G-) MDSC infiltration in 4T1 tumor microenvironment. Cell percentages of granulocytic (D), monocytic (E) MDSC and TAM (F). NK cell activation (G,H) and CD8 (I) cell activation was determined using the CD107a degranulation marker. CD8 + T cell exhaustion was also measured using PD1 (J). (K) Schematic diagram of treatment (black arrows) and CD8 depletion (red arrows) schedule for 4T1 bearing mice. Treatment scheduled was the same as previously but 1 day before treatment 500 µg of CD8 depleting antibody was given and then every 2 days 100 µg was given. (L) CD8 and CD4 cell staining on CD3 gated peripheral blood from mice treated with or without depleting CD8 antibody. (M) Summary data for average tumor growth for all treatment groups for CD8 depleted 4T1 tumor model. (N) Kaplan-Meier survival curve for the treatment groups for CD8 depleted 4T1 bearing mice. MDSC, myeloid-derived suppressor cell; TAM, tumor-associated macrophage.

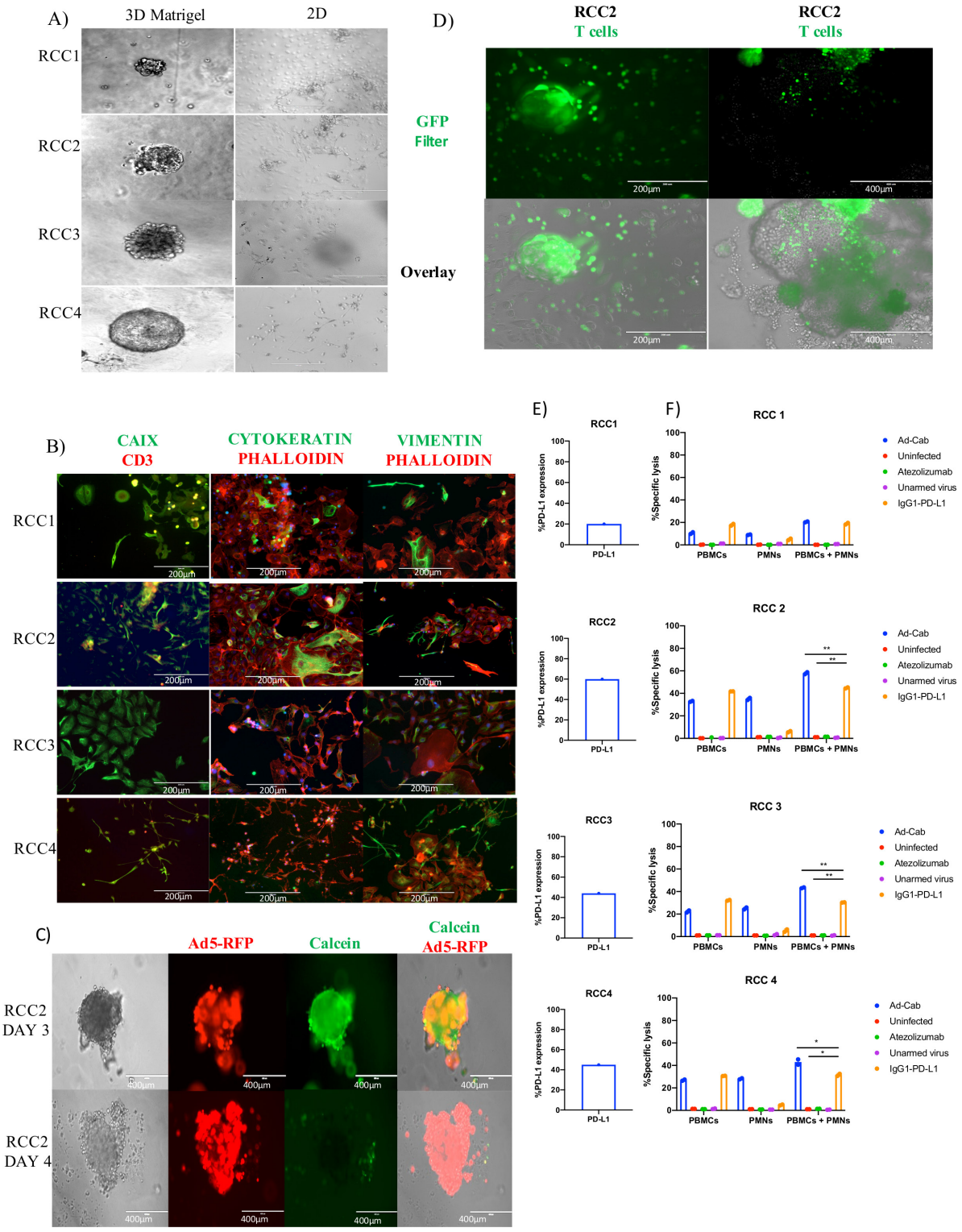

Figure 7 Characterization of Ad-Cab in RCC patient-derived organoids. (A) Representative imaging of renal cancer cell tissue grown in Matrigel as 3D (left) and 2D (right). Immunofluorescence staining of dissociated RCC PDOs using CAIX, Cytokeratin, Vimentin, CD3 and Phalloidin. Scale bar 500 or 200 µm. (C) RCC2 PDOs were infected with 5×10^5 vp of Ad5-RFP Δ24. Cell viability was visualized using Calcein green. Scale bars 200 µm. (D) Images of RCC2 PDOs infiltrated by Calcein green stained PBMCs. 10^5 PBMCs, stained with Calcein green, were added on top of Matrigel and after 4 hours images were taken using an EVOS FL cell imaging system. Scale bars 400 or 200 µm. (E) FACS analysis of PD-L1 expression of dissociated RCC PDOs. (F) ADCC assays with RCC1, RCC2, RCC3 and RCC4 PDOs. RCC PDOs were infected with viruses at 100 MOI and incubated for 48 hours or 10 µg/mL of antibody were added 30 min prior to adding immune components. PBMCs and PMNs were added at an E:T ratio of 40:1 and 100:1, respectively. LDH release assays were performed 4 hours after addition of immune effector cells. ADCC, antibody-dependent cell cytotoxicity; PBMC, peripheral blood mononuclear cell; PDO, patient-derived organoid; PMN, polymorphonuclear; RCC, renal cell carcinoma.

Varying levels of expression of CD3-/PD-L1 +positive cell were shown from the samples, from 20% to 66%. Hence, we demonstrate that the RCC PDOs can be used as testing platforms for the Ad-Cab virus, and since they express PD-L1, they can be infected by oncolytic adenoviruses and infiltrated by PBMCs.

After optimizing the RCC organoids as a functional testing platform for the Ad Cabs, we used them to perform the ADCC experiments with PBMCs and PMNs (figure 7F). RCC organoids were first infected with the viruses or treated with the antibodies and incubated for 3 days. As evident from the ADCC results, when PBMCs were added to the organoids, similar levels of cytotoxicity were observed with the Ad-Cab and the IgG1 PD-L1 antibody. Consistent with in vitro data, cytotoxicity could only be observed with the Ad-Cab and not with the IgG1 PD-L1 antibody when PMNs were added as the effector cells (figure 7F). When both populations of effector cells were added simultaneously, there was an enhanced cell killing with Ad-Cab compared with when each population was added individually (figure 7F), with all samples except RCC1 (figure 7F). This could be explained by the fact that all PD-L1 expressing cells were killed when each effector population was added individually. The added benefit of activating an additional effector population with Ad-Cab was evident since the killing efficiency in RCC2, 3 and 4 patient samples were greater when PBMCs and PMNs were added together. Thus, the PDOs further reinforced the efficacy of Ad-Cab and the significance of the synergism of the immune system for tumor eradication.

DISCUSSION

ICIs have emerged as a major clinical milestone for the treatment of cancer. However, recent data have revealed that the in vivo activity of such antibodies solely depend on the Fab-mediated inhibition of inhibitory immune checkpoints and also the effector mechanisms mediated by the Fc portion.[32–34] In this study, we designed a novel PD-L1 ICI with a cross-hybrid Fc region mediating effector mechanisms of both an IgG and an IgA. To minimize unwanted cytotoxicity, the novel ICI was cloned into a conditionally replicating adenovirus to limit release only to the tumor microenvironment. Ad-Cab secreted the cross-hybrid IgGA Fc-fusion peptide able to bind to PD-L1 and activate multiple immune pathways, not activated when IgG or IgA antibody is added alone, resulting in enhanced tumor killing in various in vitro, in vivo and ex vivo models.

As expected, the additive effector mechanisms of the Fc-fusion peptide increased tumor killing when compared with the FDA approved IgG, Atezolizumab, containing an N298A mutation abrogating Fc-γ binding. In line with other studies, the additive effector functions of the Fc-fusion peptides against PD-L1 holds potential into greater clinical results.[9 10] Based on in vitro and in vivo analysis, a crucial mechanism of action of several therapeutic antibodies against cancer is to elicit tumor cell killing via ADCC and CDC.[35] As for ICIs, including a functional Fc region may not always be beneficial and depends on the immune checkpoint receptor targeted. For example, equipping CTLA-4[8] and PD-L1 ICIs[9 10] with a competent Fc region able to elicit ADCC has been shown to enhance efficacy yet with PD-1 antibodies, it reduced efficacy. Coinciding with previous results, we also show that incorporating effector mechanisms to PD-L1 ICIs increases efficacy due to enhanced tumor killing. Our results demonstrate that mice bearing CT26 and 4T1 tumors responded better to Ad-Cab compared with mPD-L1. This superiority is hypothesized to be due to the enhanced Fc-effector mechanisms since the Fc-fusion peptide is partly human IgG1 and such isotype induces greater ADCC compared with IgG2a (isotype of mPD-L1) in mice.[12] This coincides with our data showing an enhanced activation of NK cells when treated with Ad-Cab compared with mPD-L1. Moreover, when CD8 T cells were depleted, mPDL1 was not able to control anymore the tumor growth yet Ad-Cab was able. This is mostly due to the engagement of other immune cells such as NK cells as an effector population by Ad-Cab. Other than augmenting tumor cell killing, Ad-Cab was also shown to stimulate an antitumor memory response since CT26 recovered mice treated with Ad-Cab did not engraft a second challenge of CT26. The augmented tumor cell killing could have resulted in the excess release of tumor antigens being picked up by infiltrated dendritic cells. Therefore, other than having a local impact, the increased tumor cell killing by the engagement of multiple effector population could lead to a systemic effect.

Interestingly, Ad-Cab was able to affect the tumor microenvironment by reducing highly immunosuppressive cell populations such as monocytic MDSCs and granulocytic MDSCs in 4T1 bearing mice. Such cell populations have been attributed to enhanced tumor growth, suppressing pre-existing antitumor responses and impeding the efficacy of many cancer immunotherapies. It is believed that Ad-Cab was able to reduce such immunosuppressive immune populations due to their abnormally high expression of PD-L1. Even though other myeloid cells such as dendritic cells, macrophages, monocytes or neutrophils express PD-L1, they were unharmed by Ad-Cab both in vitro and in vivo. These results fall in line with previous studies and have contributed to the number of PD-L1 molecules expressed on the cell membrane which is a key determinant for antibody effector functions. Hence, other than increasing tumor cell killing, Ad-Cab is also able to counteract suppressive immune populations highly expressing PD-L1.

Despite the fact that neutrophils express activating Fc-γIIA, able to trigger ADCC, the cells also express one log more of Fc-γIIIB.[36] Unlike other Fc-γ receptors, the Fc-γIIIB receptor does not contain either activating (ITAM) or inhibitory (ITIM) motifs and its role has been questioned. Nevertheless, with therapeutic antibodies against cancer, it has been attributed to act as a molecular “sink” by competitively binding to IgG with

no resulting activation.[12 13 37] Yet, the Fc-fusion peptide was able to capitalize on such a neglected cell population due to their high expression of Fc-α. Neutrophils are the most abundant leukocyte population in blood and tumorigenesis skews hematopoiesis towards neutrophil production by secreting granulocyte-colony stimulating factor (G-CSF) and granulocyte-macrophage-colony stimulating factor (GM-CSF) leading to tumor infiltration.[38–40] Regardless of their high tumor infiltration, these cells have shown to be protumorigenic and their tumor infiltration has been associated with a low clinical prognosis.[41] This associated low prognosis is due to the lack of effective neutrophil-activating stimulus and the immunosuppressive tumor microenvironment polarizes the cells towards pro-tumorigenic.[39] Many studies have shown that the tumor microenvironment can direct the fate of neutrophils towards either antitumorigenesis or protumorigenesis.[42–44] Hence, the ability of Fc-fusion peptide to activate neutrophils can polarize already tumor-infiltrated neutrophils from tumor-promoting to tumor-killing cells. Subsequently, the activation of neutrophils can lead to the release of multiple cytokines and chemokines to recruit other effector immune cells[45] that the Fc-fusion peptide can further activate. Unfortunately, since mice do not express endogenous Fc-alpha receptors, the full efficacy of Ad-Cab could not be studied in vivo. In the future, transgenic mice expressing Fc-alpha receptors should be used to fully assess the efficacy of Ad-Cab. Other than eliminating, it would be interesting to examine whether the activation of Fc-alpha receptors on granulocytic or monocytic MDSC could help polarize such cell to be antitumorigenic.

To extensively evaluate the efficacy of the Fc-fusion peptide, we used RCC PDOs. PDOs have revolutionized the study of cancer since analysis of patient-derived tissue can be done without invasive procedures. Additionally, PDO cultures have allowed to test individual responses of patients ex vivo with a high sensitivity and specificity in multitude types of tumors.[46 47] This is because the PDOs can mimic tumor heterogeneity with respect to genetics and architecture often lacking with in vitro cell lines and animal models.[48] To our knowledge, currently there are only two published studies that have evaluated the efficacy of oncolytic viruses using PDOs.[49 50] This is the first study where the efficacy of the oncolytic virus was tested and an ADCC assay was performed. PDO data further demonstrated the added efficacy of the Fc-fusion peptide by eliciting ADCC with PBMCS and PMNs. This dual activation of both populations was also shown to augment tumor killing compared with when each population was added individually, or one population was only activated by the IgG1 PD-L1. Hence, these data have broadly evaluated the preclinical efficacy of the Fc-fusion peptide.

This synergistic effect by simultaneously engaging Fc-α and Fc-γ was also shown by Brandsma and colleagues,[17] when IgA and IgG antibodies against two different tumor-associated antigens (TAAs) were added and a higher tumor killing was observed compared with when each antibody was used individually. Interestingly, this effect was only seen when the antibodies were directed towards two different TAAs and diminished when they were directed towards the same TAA. From data presented in this study, it can be deduced that this diminished effect could have been due to the competitive binding between the IgG and IgA antibodies towards the same epitope, since this synergistic effect was shown in the Fc-fusion peptide that incorporated both an IgG and IgA.

In conclusion, here we demonstrate a novel ICI, with enhanced tumor killing efficacy, expressed from an oncolytic adenovirus to limit toxicities. We have shown that the Fc-fusion peptide is able to activate PBMCs, usually activated by IgG1 antibodies, and engage a neglected but important population, PMNs. This coengagement of both populations was shown to work in synergy augmenting tumor killing in various PD-L1 expressing cell lines and RCC PDOs. Such preclinical results prompt the further investigation of Ad-Cab towards the path of clinical development.

Author affiliations
[1]Laboratory of Immunovirotherapy, Drug Research Program, University of Helsinki Faculty of Pharmacy, Helsinki, Uusimaa, Finland
[2]TRIMM, Translational Immunology Research Program, University of Helsinki, Helsinki, Uusimaa, Finland
[3]Drug Delivery, Drug Research Program, Division of Pharmaceutical Biosciences, Faculty of Pharmacy, University of Helsinki, Helsinki, Finland
[4]Translational Stem Cell Biology & Metabolism Program, Research Programs Unit, Department of Anatomy, Faculty of Medicine, Biomedicum Helsinki, University of Helsinki, Helsinki, Finland
[5]Hematology Research Unit Helsinki, University of Helsinki, Helsinki, Uusimaa, Finland
[6]Abdominal Center, Urology, Helsinki University Central Hospital, Helsinki, Uusimaa, Finland
[7]Center for Translational Immunology, UMC Utrecht, Utrecht, Netherlands
[8]iCAN Digital Precision Cancer Medicine Flagship, University of Helsinki, Helsinki, Finland
[9]Department of Clinical Chemistry and Hematology, University of Helsinki, Helsinki, Finland
[10]Department of Anatomy, University of Helsinki, Helsinki, Finland
[11]Department of Molecular Medicine and Medical Biotechnology and CEINGE, Naples University 24 Federico II, 80131, Naples, Italy

Correction notice This paper has been updated since first published to amend author name 'Moon Hee Lee'.

Twitter Satu Mustjoki @hruh_research and Vincenzo Cerullo @vincersurf

Acknowledgements We thank H Ibrahim for helping us with live cell microscopy. We also thank L Pietilä for helping us with collecting serum.

Contributors FH, EY, JC and VC conceived and planned all the experiments. FH and YG carried out most of the experiments. EY, MF, SF, JC, BM, MF, SR, OKK, AK and MG helped in carrying out most of the experiments. ML and TGM helped in carrying out live-cell microscopy. ML, PJ, HN, AK, MG and SM helped with providing patient material and conducting related experiments. MG and VC supervised the project. FH, EY, MG and VC wrote and corrected the paper. All authors provided critical feedback and helped shape the research, analysis and manuscript.

Funding FH thanks the Research Foundation of the University of Helsinki for funding his doctoral studies at the Faculty of Pharmacy, Helsinki University. VC acknowledges the European Research Council under the Horizon 2020 framework (https://erc.europa.eu), ERC-consolidator Grant (Agreement no. 681219), Jane and Aatos Erkko Foundation (Project no. 4705796), HiLIFE Fellow (Project no. 797011004), Cancer Finnish Foundation (Project no. 4706116), Magnus Ehrnrooth Foundation (Project no. 4706235), Academy of Finland and Digital Precision Cancer Medicine Flagship iCAN. SM received funding from the Cancer Foundation

Finland, the Sigrid Juselius Foundation, the Relander Foundation, state funding for university-level research in Finland and HiLife fellow funds from the University of Helsinki.

Competing interests None declared.

Patient consent for publication Not required.

Ethics approval This study was approved by the Helsinki University Hospital Ethical committee (Renal Cell Carcinoma patients DNRO 115/13/03/02/15).

Provenance and peer review Not commissioned; externally peer reviewed.

Data availability statement All data relevant to the study are included in the article or uploaded as supplementary information. All data relevant to the study are included in the article or uploaded as supplementary information.

ORCID iDs
Firas Hamdan http://orcid.org/0000-0003-4678-7382
Erkko Ylösmäki http://orcid.org/0000-0001-9678-2614
Manlio Fusciello http://orcid.org/0000-0002-7166-3018
Sara Feola http://orcid.org/0000-0002-4012-4310
Jeanette Leusen http://orcid.org/0000-0003-4982-6914
Satu Mustjoki http://orcid.org/0000-0002-0816-8241
Vincenzo Cerullo http://orcid.org/0000-0003-4901-3796

REFERENCES

1 Hodi FS, O'Day SJ, McDermott DF, *et al*. Improved survival with ipilimumab in patients with metastatic melanoma. *N Engl J Med* 2010;363:711–23.
2 Tsao H, Atkins MB, Sober AJ. Management of cutaneous melanoma. *N Engl J Med Overseas Ed* 2004;351:998–1012.
3 Zhang B, Song Y, Fu Y, *et al*. Current status of the clinical use of PD-1/PD-L1 inhibitors: a questionnaire survey of oncologists in China. *BMC Cancer* 2020;20:86.
4 Topalian SL, Sznol M, McDermott DF, *et al*. Survival, durable tumor remission, and long-term safety in patients with advanced melanoma receiving nivolumab. *J Clin Oncol* 2014;32:1020–30.
5 Pardoll DM. The blockade of immune checkpoints in cancer immunotherapy. *Nat Rev Cancer* 2012;12:252–64.
6 Chen X, Song X, Li K, *et al*. FcγR-Binding is an important functional attribute for immune checkpoint antibodies in cancer immunotherapy. *Front Immunol* 2019;10:292.
7 Brezski RJ, Georgiou G. Immunoglobulin isotype knowledge and application to Fc engineering. *Curr Opin Immunol* 2016;40:62–9.
8 Simpson TR, Li F, Montalvo-Ortiz W, *et al*. Fc-Dependent depletion of tumor-infiltrating regulatory T cells co-defines the efficacy of anti-CTLA-4 therapy against melanoma. *J Exp Med* 2013;210:1695–710.
9 Dahan R, Sega E, Engelhardt J, *et al*. FcγRs modulate the anti-tumor activity of antibodies targeting the PD-1/PD-L1 axis. *Cancer Cell* 2015;28:285–95.
10 Goletz C, Lischke T, Harnack U, *et al*. Glyco-engineered anti-human programmed death-ligand 1 antibody mediates stronger CD8 T cell activation than its normal glycosylated and non-glycosylated counterparts. *Front Immunol* 2018;9.
11 Bournazos S, Wang TT, Ravetch JV. The role and function of Fcγ receptors on myeloid cells. *Microbiol Spectr* 2016;4.
12 Treffers LW, van Houdt M, Bruggeman CW, *et al*. Fcγriiib restricts antibody-dependent destruction of cancer cells by human neutrophils. *Front Immunol* 2018;9:3124.
13 Derer S, Glorius P, Schlaeth M, *et al*. Increasing FcγRIIa affinity of an FcγRIII-optimized anti-EGFR antibody restores neutrophil-mediated cytotoxicity. *MAbs* 2014;6:409–21.
14 Brandsma AM, Bondza S, Evers M, *et al*. Potent Fc receptor signaling by IgA leads to superior killing of cancer cells by neutrophils compared to IgG. *Front Immunol* 2019;10.
15 Lohse S, Brunke C, Derer S, *et al*. Characterization of a Mutated IgA2 Antibody of the m(1) Allotype against the Epidermal Growth Factor Receptor for the Recruitment of Monocytes and Macrophages. *J Biol Chem* 2012;287:25139–50.
16 Dechant M, Valerius T. Iga antibodies for cancer therapy. *Crit Rev Oncol Hematol* 2001;39:69–77.
17 Brandsma AM, Ten Broeke T, Nederend M, *et al*. Simultaneous targeting of FcγRs and FcαRI enhances tumor cell killing. *Cancer Immunol Res* 2015;3:1316–24.
18 Kelton W, Mehta N, Charab W, *et al*. IgGA: A "cross-isotype" engineered human Fc antibody domain that displays both IgG-like and IgA-like effector functions. *Chem Biol* 2014;21:1603–9.
19 Feng Y, Roy A, Masson E, *et al*. Exposure-Response relationships of the efficacy and safety of ipilimumab in patients with advanced melanoma. *Clin Cancer Res* 2013;19:3977–86.
20 Dias JD, Hemminki O, Diaconu I, *et al*. Targeted cancer immunotherapy with oncolytic adenovirus coding for a fully human monoclonal antibody specific for CTLA-4. *Gene Ther* 2012;19:988–98.
21 Höti N, Li Y, Chen C-L, *et al*. Androgen receptor attenuation of Ad5 replication: implications for the development of conditionally replication competent adenoviruses. *Mol Ther* 2007;15:1495–503.
22 Nemunaitis J, Tong AW, Nemunaitis M, *et al*. A phase I study of telomerase-specific replication competent oncolytic adenovirus (telomelysin) for various solid tumors. *Mol Ther* 2010;18:429–34.
23 Kanerva A, Zinn KR, Chaudhuri TR, *et al*. Enhanced therapeutic efficacy for ovarian cancer with a serotype 3 receptor-targeted oncolytic adenovirus. *Mol Ther* 2003;8:449–58.
24 Hamdan F, Martins B, Feodoroff M, *et al*. GAMER-Ad: a novel and rapid method for generating recombinant adenoviruses. *Mol Ther Methods Clin Dev* 2021;20:625-634.
25 Maute RL, Gordon SR, Mayer AT, *et al*. Engineering high-affinity PD-1 variants for optimized immunotherapy and immuno-PET imaging. *Proc Natl Acad Sci U S A* 2015;112:E6506–14.
26 Treffers LW, Ten Broeke T, Rösner T, *et al*. IgA-Mediated killing of tumor cells by neutrophils is enhanced by CD47–SIRPA checkpoint inhibition. *Cancer Immunol Res* 2020;8:120–30.
27 Matlung HL, Babes L, Zhao XW, *et al*. Neutrophils kill Antibody-Opsonized cancer cells by Trogoptosis. *Cell Rep* 2018;23:3946–59.
28 Garcia-Diaz A, Shin DS, Moreno BH, *et al*. Interferon receptor signaling pathways regulating PD-L1 and PD-L2 expression. *Cell Rep* 2017;19:1189–201.
29 Dosset M, Vargas TR, Lagrange A, *et al*. Pd-1/Pd-L1 pathway: an adaptive immune resistance mechanism to immunogenic chemotherapy in colorectal cancer. *Oncoimmunology* 2018;7:e1433981.
30 Sagiv-Barfi I, Kohrt HEK, Czerwinski DK, *et al*. Therapeutic antitumor immunity by checkpoint blockade is enhanced by ibrutinib, an inhibitor of both BTK and ITK. *Proc Natl Acad Sci U S A* 2015;112:E966–72.
31 Yu W, Wang Y, Jiang Y, *et al*. Distinct immunophenotypes and prognostic factors in renal cell carcinoma with sarcomatoid differentiation: a systematic study of 19 immunohistochemical markers in 42 cases. *BMC Cancer* 2017;17.
32 Chan HTC, Hughes D, French RR, *et al*. CD20-induced lymphoma cell death is independent of both caspases and its redistribution into Triton X-100 insoluble membrane rafts. *Cancer Res* 2003;63:5480–9.
33 Diebolder CA, Beurskens FJ, de Jong RN, *et al*. Complement is activated by IgG hexamers assembled at the cell surface. *Science* 2014;343:1260–3.
34 Nimmerjahn F, Ravetch JV. Fcgamma receptors as regulators of immune responses. *Nat Rev Immunol* 2008;8:34–47.
35 Desjarlais JR, Lazar GA. Modulation of antibody effector function. *Exp Cell Res* 2011;317:1278–85.
36 Wang Y, Jönsson F. Expression, role, and regulation of neutrophil Fcγ receptors. *Front Immunol* 2019;10:1958.
37 Peipp M, Lammerts van Bueren JJ, Schneider-Merck T, *et al*. Antibody fucosylation differentially impacts cytotoxicity mediated by NK and PMN effector cells. *Blood* 2008;112:2390–9.
38 Kowanetz M, Wu X, Lee J, *et al*. Granulocyte-Colony stimulating factor promotes lung metastasis through mobilization of Ly6G+Ly6C+ granulocytes. *Proc Natl Acad Sci U S A* 2010;107:21248–55.
39 Casbon A-J, Reynaud D, Park C, *et al*. Invasive breast cancer reprograms early myeloid differentiation in the bone marrow to

generate immunosuppressive neutrophils. *Proc Natl Acad Sci U S A* 2015;112:E566–75.
40 Coffelt SB, Kersten K, Doornebal CW, *et al*. Il-17-Producing γδ T cells and neutrophils conspire to promote breast cancer metastasis. *Nature* 2015;522:345–8.
41 Wang J, Bo X, Suo T, *et al*. Tumor-Infiltrating neutrophils predict prognosis and adjuvant chemotherapeutic benefit in patients with biliary cancer. *Cancer Sci* 2018;109:2266–74.
42 Braster R, O'Toole T, van Egmond M. Myeloid cells as effector cells for monoclonal antibody therapy of cancer. *Methods* 2014;65:28–37.
43 Albanesi M, Mancardi DA, Jönsson F, *et al*. Neutrophils mediate antibody-induced antitumor effects in mice. *Blood* 2013;122:3160–4.
44 Uchida J, Hamaguchi Y, Oliver JA, *et al*. The innate mononuclear phagocyte network depletes B lymphocytes through Fc receptor-dependent mechanisms during anti-CD20 antibody immunotherapy. *J Exp Med* 2004;199:1659–69.
45 Mantovani A, Cassatella MA, Costantini C, *et al*. Neutrophils in the activation and regulation of innate and adaptive immunity. *Nat Rev Immunol* 2011;11:519–31.
46 Maru Y, Tanaka N, Itami M, *et al*. Efficient use of patient-derived organoids as a preclinical model for gynecologic tumors. *Gynecol Oncol* 2019;154:189–98.
47 Boj SF, Hwang C-I, Baker LA, *et al*. Organoid models of human and mouse ductal pancreatic cancer. *Cell* 2015;160:324–38.
48 Fusco P, Parisatto B, Rampazzo E, *et al*. Patient-Derived organoids (PDOs) as a novel in vitro model for neuroblastoma tumours. *BMC Cancer* 2019;19.
49 Heideman DAM, Steenbergen RDM, van der Torre J, *et al*. Oncolytic adenovirus expressing a p53 variant resistant to degradation by HPV E6 protein exhibits potent and selective replication in cervical cancer. *Molecular Therapy* 2005;12:1083–90.
50 Zhu Z, Gorman MJ, McKenzie LD, *et al*. Zika virus has oncolytic activity against glioblastoma stem cells. *J Exp Med* 2017;214:2843–57.